J. theor. Biol. (1985) **113**, 163–223

A Neural Theory of Circadian Rhythms: Split Rhythms, After-effects and Motivational Interactions

GAIL A. CARPENTER†

Department of Mathematics, Northeastern University, Boston and Center for Adaptive Systems, Department of Mathematics, Boston University, Boston, Massachusetts 02215, *U.S.A.*

AND

STEPHEN GROSSBERG‡

Center for Adaptive Systems, Department of Mathematics, Boston University, Boston, Massachusetts 02215, *U.S.A.*

(*Received* 26 *April* 1984, *and in revised form* 25 *October* 1984)

A neural theory of the circadian pacemaker within the hypothalamic suprachiasmatic nuclei (SCN) is used to explain parametric data about mammalian operant behavior. The intensity, duration, and patterning of ultradian activity-rest cycles and the duration of circadian periods due to parametric (LL) and nonparametric (LD) lighting regimes are simulated. Paradoxical data about split rhythms and after-effects are explained using homeostatic and nonhomeostatic neural mechanisms that modulate pacemaker activity. These modulatory mechanisms enable the pacemaker to adjust to pervasive changes in its lighting regime, as during the passage of seasons, and to ultradian changes in internal metabolic conditions. The model circadian mechanisms are homologous to mechanisms that model hypothalamically mediated appetitive behaviors, such as eating. The theory thus suggests that both circadian and appetitive hypothalamic circuits are constructed from similar neural components. Mechanisms of transmitter habituation, opponent feedback interactions between on-cells and off-cells, homeostatic negative feedback, and conditioning are used in both the circadian and the appetitive circuits. Output from the SCN circadian pacemaker is assumed to modulate the sensitivity of the appetitive circuits to external and internal signals by controlling their level of arousal. Both underarousal and overarousal can cause abnormal behavioural syndromes whose properties have been found in clinical data. A model pacemaker can also be realized as an intracellular system.

† Supported in part by the National Science Foundation (NSF MCS-82-07778) and the Office of Naval Research (ONR-N0014-83-KO337).

‡ Supported in part by the Office of Naval Research (ONR-N0014-83-KO337).

0022-5193/85/050163+61 $03.00/0

© 1985 Academic Press Inc. (London) Ltd

1. Introduction: A Neural Model of the Circadian System in the Mammalian Suprachiasmatic Nuclei

A circadian pacemaker that helps to control the wake-sleep and activity-rest cycles of mammals has been identified in the suprachiasmatic nuclei (SCN) of the hypothalamus (Hedberg & Moore-Ede, 1983; Inouye & Kawamura, 1979; Moore, 1973, 1974; Moore & Eichler, 1972; Stephan & Zucker, 1972). A neural model of this SCN circadian system has recently been developed (Carpenter & Grossberg, 1982, 1983*a,b*, 1984). This model, called the gated pacemaker, was constructed from neural components that have also been used to model motivated behaviors, such as eating and drinking, that are controlled by other hypothalamic circuits (Grossberg, 1972*a,b*, 1975, 1982*a,b*, 1984*a*; Olds, 1977). Thus our SCN model forms part of a larger theory of how hypothalamic circuits may be specialized to control different types of motivated behaviors.

The gated pacemaker model of the SCN has been used to quantitatively simulate a large body of circadian data. These data include Aschoff's rule in nocturnal and diurnal mammals (Aschoff, 1960) and exceptions to Aschoff's rule in diurnal mammals (Aschoff, 1979); the circadian rule in nocturnal and diurnal mammals (Aschoff, 1960); the tendency of nocturnal mammals to lose circadian rhythmicity at lower light levels than diurnal mammals (Aschoff, 1979); the suppression of circadian rhythmicity by bright light (Aschoff, 1979; Enright, 1980); the increase of circadian period during a self-selected light-dark cycle in diurnal mammals (Aschoff, 1979; Wever, 1979); and the phase response curves to pulses of light in diurnal and noctural mammals, including the "dead zone" of phase resetting insensitivity during the subjective day of a nocturnal mammal (Daan & Pittendrigh, 1976; DeCoursey, 1960; Kramm, 1971; Pohl, 1982). Due to the fact that every process in the model has a physical interpretation, the model suggests a number of anatomical, physiological, and pharmacological predictions to test its validity. Notable among these are predictions that test whether slowly varying transmitter gating actions form part of the SCN pacemaker. In model circuits controlling motivated behaviors such as eating and drinking, such slow gating processes have been used to analyse a variety of abnormal behaviors, such as juvenile hyperactivity, Parkinsonism, hyperphagia, and simple schizophrenia (Grossberg, 1972*b*, 1984*a,b*). If a slow gating action is verified in the SCN, it would provide a new basis for analysing certain abnormalities of circadian rhythms and their effects on the motivational circuits that they modulate.

This article suggests an explanation of several types of long-term after-effects (Aschoff, 1979; Pittendrigh, 1960, 1974; Pittendrigh & Daan, 1976*a*), split rhythms (Earnest & Turek, 1982; Hoffmann, 1971; Pittendrigh, 1960;

Pittendrigh & Daan, 1976*b*), and SCN ablation studies (Pickard & Turek, 1982). We also note a functional similarity that exists between the SCN pacemaker model and a model of the transduction of light by vertebrate photoreceptors (Carpenter & Grossberg, 1981). This comparison suggests how photoreceptor mechanisms may be modified to form retinal circadian pacemakers, as in the isolated eye of *Aplysia* (Jacklet, 1969) and the frog *Xenopus laevis* (Iuvone, Besharse & Dunis, 1983). The models of vertebrate photoreceptor, SCN circadian pacemaker, and hypothalamic motivational circuits are all variations of a neural network design called a *gated dipole* (Grossberg, 1972*b*, 1975). Gated dipoles model opponent processes wherein slowly accumulating chemical transmitters are depleted, or habituated, by gating signals which are energized by tonic arousal and phasic inputs.

The gated pacemaker model has a neurophysiological interpretation as the neural pacemaker within the mammalian SCN. Most models of circadian rhythms have assumed a classical oscillator, such as a van der Pol or FitzHugh-Nagumo oscillator (Kawato & Suzuki, 1980; Kronauer *et al.*, 1982) as their starting point. Other approaches replace an analysis of pacemaker dynamics by formal algebraic or stochastic rules that govern phase relationships (Daan & Berde, 1978; Enright, 1980). Such models focus upon how couplings between two oscillators, or populations of oscillators, can stimulate circadian properties.

Our theory focusses instead upon the physiological characterization of each oscillator and upon the circadian properties of a single population of these oscillators.

In other approaches, circadian properties are explained in terms of the phase differences between oscillators. Our analysis suggests that circadian properties, such as long-term after-effects (section 3) and aspects of split rhythms (section 10), which were thought to be necessarily due to two or more out-of-phase oscillators, can be generated by a single population of in-phase oscillators. Our analysis also suggests that the two-oscillator explanations of split rhythm and after-effect data are in need of revision (sections 3 and 23). The gated pacemaker model is not, however, incompatible with the idea that certain split rhythms may occur when individual pacemakers drift out-of-phase. In fact, the gated pacemaker model postulates the existence of modulatory processes which, among other roles, may better entrain pacemaker cells under certain experimental conditions than others. We now describe these modulatory processes.

2. Homeostatic and Nonhomeostatic Modulators of the Circadian Pacemaker

In order to simulate split rhythm and after-effect data using a single in-phase pacemaker population, we introduce processes which homeostatic-

ally and nonhomeostatically modulate the circadian pacemaker. These modulatory processes are distinct from the pacemaker mechanism *per se*. Analogous modulatory processes are known to regulate hypothalamically controlled appetitive behaviors such as eating (Grossberg, 1984*a*, 1985).

For example, eating behavior is modulated by internal homeostatic influences, such as satiety signals, that build up on an ultradian time scale. These homeostatic influences prevent undue gastric distention and metabolic overload from occurring due to unrestricted eating behavior. We assume that a homeostatic feedback signal also modulates the circadian pacemaker on an ultradian time scale. This negative feedback signal serves as a metabolic index of fatigue (Carpenter & Grossberg, 1982, 1983*a*, 1984) which is suggested to reach the pacemaker via the bloodstream. The fatigue signal acts on all the oscillators in the pacemaker circuit. It can thus act as an internal Zeitgeber that synchronizes these pacemakers as it also modulates their activity level through time. This internal Zeitgeber has the same formal properties as the sleep-dependent Process S that was discovered by Borbély (1982) using EEG methods. The EEG techniques of Borbély provide an independent experimental procedure for testing properties of the fatigue signal. A variety of substances in the bloodstream may contribute to the total fatigue signal. This observation suggests that many types of receptors may exist in SCN cells to sense the total fatigue signal. Alternatively, a single chemical signal may reach the SCN after being released due to the action of many bloodstream substances, or other processes, upon a different brain region. Our theory suggests that the chemical receptors which sense the fatigue signal are not part of the pacemaker mechanism *per se*. The formal homolog between the ultradian satiety and fatigue signals also suggests the possibility that some chemical components of both signals may be the same. More generally, this homolog may be related to clinical correlations between eating and sleeping disorders.

A perfect internal homeostatic control of eating would badly serve an animal's survival if it could not be modulated by external signals of food availability and quality. Consequently the eating behavior of many mammals is also influenced by nonhomeostatic constraints. These nonhomeostatic constraints include oropharyngeal factors, such as taste, which endow food-predictive cues with their gustatory appeal. They also include reinforcing events which enable indifferent cues, such as the sight of food, to act as effective predictors of food. Both types of nonhomeostatic factors can override homeostatic constraints to enable a mammal to eat when food becomes available. Oropharyngeal factors, such as taste, act on a fast time scale. By contrast, reinforcement can have effects that persist on a much slower time scale.

We suggest that fast and slow nonhomeostatic factors also modulate activity within the SCN circadian pacemaker. The fast nonhomeostatic factor describes the influence of the momentary patterning of light within the experimental chamber upon the SCN pacemaker. We distinguish between the light intensity within the experimental chamber and the actual effects of light upon the pacemaker. In particular, the attentuation of light input to the pacemaker during sleep due, for example, to eye closure, retreat to a dark nest, or self-selected light-dark cycles, plays an important role in our explanation of violations of Aschoff's rule in diurnal mammals (Aschoff, 1979; Carpenter & Grossberg, 1984) and of the "dead zone" during the subjective day of a nocturnal mammal (Carpenter & Grossberg, 1983*b*; Pohl, 1982). Our explanations of split rhythms and long-term after-effects in this article also use a real-time light input to the pacemaker. Previous explanations of these data have postulated distinct mechanisms for processing constant and non-constant experimental light sources (Daan & Berde, 1978; Pittendrigh & Daan, 1976*a*). These mechanisms are incompatible with light attentuation factors (sections 3 and 23).

The slow nonhomeostatic factor modulates pacemaker activity in response to statistically reliable lighting changes, such as seasonal fluctuations, and buffers the pacemaker against adventitious lighting changes, such as cloudy weather. This slowly varying gain control process thus acts like a third type of Zeitgeber to the pacemaker. The gain control signal is physically interpreted in terms of factors that control the production and release of a chemical transmitter substance. In the model eating circuit, homologous gain control signals control the conditioned reinforcing properties of food-related cues.

Four distinct chemically mediated processes are thus used to define the SCN model. Each of these processes normally functions on a different time scale: the rapid light signal; the ultradian fatigue signal; the circadian pacemaker gating signal; and the slow gain control signal. The time scales on which these signals normally oscillate within the model do not necessarily equal the time scales of the model's reaction to experimental application of chemical agonists. A rapid phase shift in the circadian rhythm could, for example, be caused by applying an agonist of the transmitter that controls the slow gain control process.

A possible chemical interpretation of these transmitter systems is suggested by comparing the gated pacemaker model with the homologous model circuit that is used to analyse hypothalamically controlled eating behavior. In the eating circuit, for example, the transmitter system that is homologous to the slow gain control transmitter is interpreted as a cholinergic transmitter. Earnest & Turek (1983) have reported that carbachol, a

cholinergic agonist, can rapidly phase shift the SCN pacemaker. In order to determine whether carbachol is activating the slow nonhomeostatic gain control pathway, or a fast nonhomeostatic pathway that is directly activated by light (Earnest & Turek, 1983), or both, locally applied cholinergic inhibitors might be useful. Suppose, for example, that the circadian rhythm is phase shifted by light, but no longer by carbachol, after a suitable local application of a cholinergic inhibitor. Then a long-term after-effect experiment could test whether or not the slow gain control process is cholinergic. If no long-term after-effects are generated (section 3), then the cholinergic system in question may be part of the slow gain control pathway. This experimental strategy can be used to characterize the slow gain control transmitter even if its turns out not to be cholinergic.

A gated pacemaker model can also be realized as an intracellular system in which opponent membrane interactions play the role of on-cells and off-cells (section 22).

3. Long-term After-effects: Parametric and Nonparametric Experiments

Concerning long-term after-effects, Pittendrigh (1974) has written "They are more widespread than the current literature suggests; they are not accounted for by any of the several mathematical models so far published; and they must be reckoned with in the mechanisms of entrainment" (p. 441). Again in 1976, Pittendrigh & Daan (1976*a*, p. 234) wrote: "The literature has paid little attention to after-effects in the 15 years since they were first reported".

Long-term after-effects are changes in activity and/or period that persist in the dark after their inducing light regimes are terminated (Pittendrigh, 1960). These changes can persist for months. Long-term after-effects with ostensibly contradictory properties are caused by parametric and nonparametric light regimes. A parametric light regime is one in which a steady light is maintained for a number of days before the animal free-runs in the dark. A nonparametric light regime is one in which light and dark intervals alternate for a number of days before the animal free-runs in the dark.

The main paradox that is raised by parametric and nonparametric light regimes is summarized in Table 1. After stating the paradox, we will describe related data and our simulations of long-term after-effect data.

In Table 1 the notation LD $M:N$ means that a nocturnal mammal is placed in M hours of light followed by N hours of darkness for a number of days before being allowed to free-run in the dark (DD). The notation LL means that the animal is run in steady light for a number of days before being allowed to free-run in the dark. The notation τ_{DD} stands for the circadian period during free-run in the dark.

TABLE

	After-effect
LD 1:23	larger τ_{DD}
LD 18:6	smaller τ_{DD}
LD 12:12	smaller τ_{DD}
LL	larger τ_{DD}

(After Pittendrigh & Daan, 1976*a*).

A comparison between the nonparametric cases LD 1:23 and LD 18:6 shows that more light (case LD 18:6) causes a smaller τ_{DD} in most cases. The main parametric result is derived from comparing the parametric case LL with the nonparametric case LD 12:12. Although case LL exposes the animal to more light, the subsequent period τ_{DD} is larger than after LD 12:12. Why does the total amount of light have opposite effects on τ_{DD} after parametric vs. nonparametric light regimes?

Pittendrigh & Daan (1976*a*) claim that the differences between parametric and nonparametric after-effects are due to the onsets and offsets of light in the nonparametric (LD), but not the parametric (LL), paradigms. They write (pp. 242-243): "By definition we must conclude that the lengthening of τ in constant illumination is due to a parametric effect on the pacemaker: no change in external conditions occurs throughout its cycle. The after-effect of photoperiod is surprising only if we assume that the parametric action of a long light pulse (photoperiod) is its dominant effect. In *Drosophila pseudoobscura* the characteristically different effect of each photoperiod on the circadian pacemaker can be accounted for by the interaction of the two nonparametric effects due to the transitions at the beginning and end of each photoperiod (Pittendrigh & Minis, 1964) . . . [T]he after-effect of photoperiod on our rodent pacemakers is similarly attributable to the interaction of nonparametric effects at the beginning and end of the photoperiod."

Although LL is "by definition" parametric at the light source, LL does not necessarily have a "parametric effect on the pacemaker". During LL, an animal periodically goes to sleep and wakes up as part of its circadian cycle. When the animal goes to sleep, eye closure or a retreat to a dark nest can cause a decrease in the light input that is registered. Similarly, when the animal wakes up, eye opening can cause an increase in the effective light input. In this sense, even the parametric LL paradigm may be experienced as a nonparametric paradigm by the nervous system. Moreover, Terman & Terman (1983) have demonstrated that sensitivity to light oscillates with a circadian rhythm in the rat. This rhythm persists after the SCN

is ablated. Thus even if external light intensity remains constant, the animal's internal sensitivity to light does not. The fact that both parametric and nonparametric light regimes may be experienced nonparametrically at central pacemakers suggests that the explanation of Pittendrigh & Daan (1976*a*) is incomplete.

Our explanation recognizes the fact that both LD and LL light regimes may be functionally nonparametric at central pacemakers. But then how can the differences between LD and LL light regimes on subsequent τ_{DD} be explained? We will focus on the fact that during an LD 18:6 regime the animal is active in the dark, whereas during an LL regime the animal is active in the light.

Figure 1 describes two simulations showing long-term after-effects of photoperiod in two versions of the nocturnal model. Just as individual animals exhibit distinct activity cycles, these different versions of the model exhibit individual differences in circadian period and the patterning of activity (dark lines) while displaying the shared qualitative properties of Table 1. The simulations in Fig. 1 illustrate the nonparametric after-effect

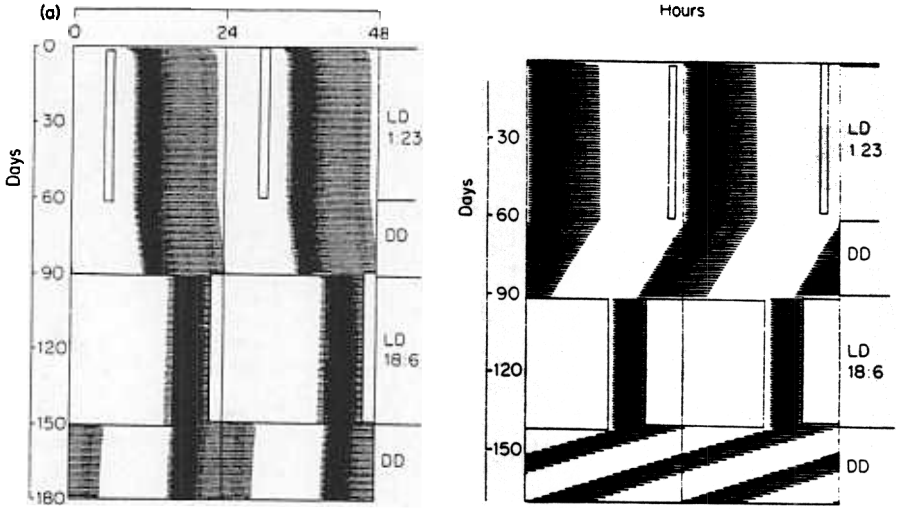

FIG. 1. Two simulations of photoperiod after-effects: In both simulations, the model is exposed to an LD 1:23 lighting regime (1 hour of light every 24 hours) before free-running in the dark. Then the model experiences an LD 18:6 lighting regime before free-running in the dark. The free-running activity levels and periods depend upon the prior lighting regimes and persist throughout the 30-day free-run intervals. Each figure is a double-plot. Two successive days are plotted in each row and each successive day is plotted in the left-hand column. Thus the day plotted in the right-hand column of the ith row is also plotted in the left-hand column of the $(i+1)$st row. Parameter values are given in the Appendix.

experiments that Pittendrigh (1974, p. 438) and Pittendrigh & Daan (1976*a*, pp. 240–243) carried out using the white-footed deermouse (*Peromyscus leucopus*). In Fig. 1(a), 1 hour of light alternated with 23 hours of darkness (LD 1:23) for 60 days. The bracketed white regions define the time intervals during which light was on. A free-run in the dark (DD) for 30 days followed. Then 18 hours of light alternated with 6 hours of darkness (LD 18:6) for 60 days. Thereafter the model free-ran in the dark for 30 days. Figure 1(b) models a similar experiment, except that LD 18:6 occurs for 50 days before the model free-runs in DD for 30 days, as in the Pittendrigh (1974) experiment.

In both simulations, the free-running period in the dark (τ_{DD}) is shorter after LD 18:6 than after LD 1:23. In Fig. 1(a), the two periods are 24·04 hours and 23·96 hours. In Fig. 1(b), the two periods are 23·7 hours and 22·7 hours. In both simulations, the duration of the active phase (dark lines) after LD 18:6 is less than the duration of the active phase after LD 1:23, as also occurs in the data.

Figure 2 describes a simulated after-effect of constant light (LL). In this parametric setting, the main effect of steady light on the white-footed

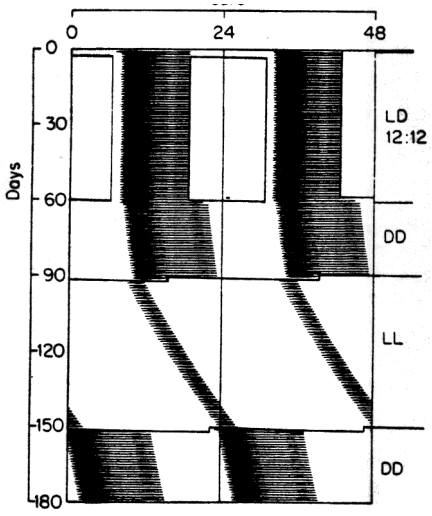

FIG. 2. Simulation of an after-effect of constant light: An LD 12:12 lighting regime followed by a free-run in the dark (DD) establishes a baseline free-run circadian period τ_{DD}. Then the model experiences constant light (LL) before again free-running in the dark. After the transition from DD to LL, the circadian period increases, as expected by Aschoff's rule for nocturnal mammals (Aschoff, 1960, 1979; Carpenter & Grossberg, 1984). The free-running period after LL is greater than after LD 12:12. Model parameters and light intensities are the same as in Fig. 1(a).

deermouse is to significantly increase the period both in the light and in the dark (Pittendrigh & Daan, 1976a, p. 239). In both the deermouse and the model, the after-effect due to an LD 12:12 nonparametric light regime was compared with the after-effect due to an LL parametric light regime. In both the animals and the simulation, the free-running period after LL exceeds the free-running period after LD 12:12.

Thus, although an increase in light duration (as in LD 1:23 vs LD 18:6) decreases circadian period in a nonparametric paradigm, an increase in light duration (as in LD 12:12 vs LL) increases circadian period in a parametric paradigm. The simulations in Figs 1 and 2 hereby reproduce the main data features described in Table 1. In Figs 1(a) and 2, the identical model and light intensity are used to simulate the nonparametric and parametric properties.

The simulated properties of Figs 1 and 2 depend upon the action of the slow gain control process $y(t)$ (section 2). The process $y(t)$ slowly averages pacemaker activity through time. Then $y(t)$ modulates the activity of the pacemaker by acting as a gain control signal. Thus process $y(t)$ is part of a feedback loop whereby past levels of pacemaker activity modulate future levels of pacemaker activity.

Different lighting regimes help to set up different patterns of pacemaker activity which, in turn, cause differential effects on the slow gain control process. For example, during the LD 18:6 regime in Fig. 1(a), the model is active in the dark, whereas during the LL regime in Fig. 2, the same model is active in the light. Note that the model is much more active in the dark during LD 18:6 than it is in the light during LL. Such a difference

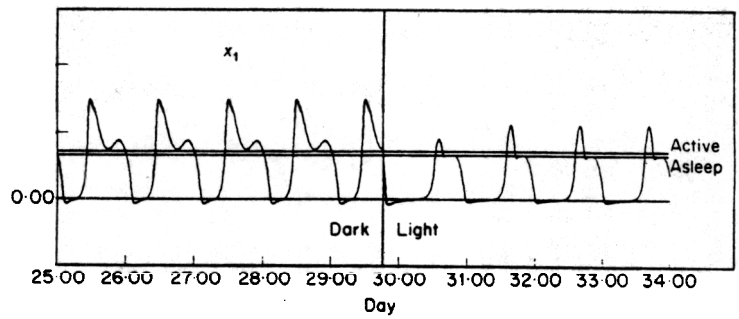

FIG. 3. Real-time plot of the pacemaker on-cell activity $x_1(t)$, defined in section 4, at the transition from DD to LL, as in Figs 2 and 10(b). The bimodal waveform during DD is compressed into a unimodal waveform during LL. This compression is due to the action of a single nonlinear oscillator, not due to the rephasing of two separate oscillators. In LL, the second, smaller portion of the bimodal wave remains near the sleep threshold.

also occurs in the data (Pittendrigh & Daan, 1976a). The differences between these activity patterns induce differences in the gain control process, which lead to the different after-effects.

Another aspect of the LD 12:12 vs LL experiments of Pittendrigh & Daan (1976*a*,*b*) is explained by our model. They write: "What these records show convincingly is that the bimodal pattern of activity in LD 12:12 is indeed produced by the same two components diverging during the DD-interval from their prior compressed state in LL" (p. 341). In Fig. 2, one can see the bimodal nature of the simulated activity pattern during LD 12:12 and DD as well as its unimodal form during LL. Figure 3 shows the time evolution of gated pacemaker activity from its bimodal form in DD to its unimodel form in LL. These simulations suggest that the unimodal form is not necessarily the compression of two separate oscillators. In the simulations, the apparent compression is due to a change in waveform of a single nonlinear oscillator.

The slow gain control process that is used to explain these parametric and nonparametric after-effects does not directly trace the pattern of light through time. The skeleton photoperiod experiments of Pittendrigh & Daan (1976*a*) show that the pattern of light alone cannot be responsible for after-effects. These experiments were run on the mouse *Mus musculus*. In such an experiment, two 1-hour light pulses are presented every 24 hours. The intervening daily dark intervals are 7 hours and 15 hours long. During this 1:7:1:15 light-dark regime, the animal is active either during the 7-hour dark interval or during the 15-hour dark interval. The initial phase of the animal's activity determines whether it will be active during the 7-hour or the 15-hour dark interval. During subsequent free-runs in the dark, the after-effect on period depends upon the phase of the animal's activity with respect to the prior lighting regime. In most cases, τ_{DD} is shorter after activity has taken place in the 7-hour dark interval than it is after activity has taken place in the 15-hour dark interval.

This result may be explained using the hypothesis that the animal's pattern of activity during a light regime, rather than the light regime itself, is a primary factor in determining properties of subsequent after-effects. For example, an animal that is active only during the 7-hour dark interval under the 1:7:1:15 regime will be active only during the 7-hour dark interval of an LD 17:7 regime. An animal that is active only during the 15-hour dark interval under the 1:7:1:15 regime will be active only during the 15-hour dark interval of an LD 9:15 regime. The size of τ_{DD} after the regimes LD 17:7 and LD 9:15 can be inferred from Table 1, where LD 18:6 and LD 1:23 are compared. From this Table, one would predict that τ_{DD} is shorter after an animal has been active during a 7-hour dark interval than after it

has been active during a 15-hour dark interval, as also occurs in the skeleton photoperiod data.

Section 7 describes in greater detail how the gain control process averages activity rather than light while it modulates pacemaker dynamics. After-effects of LD 10 : 10 vs LD 14 : 14 light regimes, which both receive 50% light during days of different duration, and of a single pulse of light will also be considered.

In contrast to the species considered above, the hamster (*Mesocricetus auratus*) does not exhibit consistent after-effects on circadian period (Pittendrigh & Daan, 1976*a*). This species does, however, exhibit split rhythms. Our explanation of split rhythms indicates why a species that exhibits split rhythms may not exhibit consistent after-effects on τ_{DD} (section 16).

4. Split Rhythms: Influences of Light, Hormones, and SCN Ablation

Pittendrigh (1960) first noted and recognized the importance of the phenomenon of *split rhythms.* Split rhythm experiments have shown that about half of all golden hamsters with a single daily activity cycle in the dark (DD) may generate an activity cycle which splits into two components in constant light (LL). Remarkably, the split does not occur until about 2 months after the hamster begins to free-run in constant light (Pittendrigh, 1974). In recent years, several examples of split rhythms have been discovered. Hoffmann (1971) described a diurnal mammal (*Tupaia belangeri*) whose rhythm splits when the level of illumination is reduced. Gwinner (1974) noted that the hormone testosterone induces split rhythms in starlings. Aschoff (1954) and Pittendrigh (1974, p. 450) also noted that "Many animals tend to be bimodal in their activity pattern" even when the activity pattern does not split.

Since Pittendrigh's original observations, many circadian models have adopted Pittendrigh's assumption that split rhythms are due to a pacemaker consisting of two or more coupled oscillators which drift out of phase when the split occurs (Daan & Berde, 1978; Gwinner, 1974; Hoffmann, 1971; Kawato & Suzuki, 1980; Moore-Ede, Sulzman & Fuller, 1982; Pittendrigh, 1974; Winfree, 1967). Wever (1962) was the first of several authors to use coupled oscillators of van der Pol type to model circadian rhythms. Our own SCN model is also built up from many oscillating components, and is compatible with results concerning desynchronization between the SCN pacemaker and a temperature pacemaker in humans (Kronauer *et al.*, 1982; Wever, 1979). We demonstrate, however, that split rhythm experiments can be simulated by our model even if its oscillating components remain in

phase. Our explanation shows how split rhythms may arise months after a change in light level, how changes in both light and hormone levels can induce splits, and how ultradian rhythms may occur even if the circadian rhythm does not split. We do not deny that certain splits may be due to out-of-phase oscillations. However, our simulations show that complex circadian waveforms are not necessarily the sum of outputs from distinct oscillators with simple (e.g. sinusoidal or van der Pol) waveforms. In a similar vein, the existence of ultradian rhythms and multimodal activity patterns does not imply the existence of an independent ultradian oscillator.

We suggest that certain split rhythms and ultradian rhythms are caused by the negative feedback signal due to fatigue, and that a slow onset of split rhythms can be traced to the slow time scale of the gain control process (section 2). Our model thus claims that certain split rhythms may be due to the joint action of two biologically useful processes. Due to the critical role of the fatigue signal in generating this type of split rhythm, we now consider the fatigue signal in greater detail.

The fatigue signal is assumed to act on the SCN pacemaker by means of substances in the bloodstream. This suggestion is consistent with electron microscopic evidence that some SCN cells are clustered in direct apposition to the walls of blood capillaries (Moore, Card & Riley, 1980; Card, Riley & Moore, 1980). Moore-Ede *et al.* (1982, p. 172) note that these cells "may act as receptors, sensing hormonal signals from elsewhere." Attributing splits to a metabolic signal though the bloodstream also suggests how injection of hormones can induce split rhythms (Gwinner, 1974). This mechanism for generating split rhythms also explains and predicts properties that are difficult for models of out-of-phase oscillators to rationalize. To understand this issue, we briefly describe the gated pacemaker model to show how the fatigue signal can, under certain circumstances, generate split rhythms.

The gated pacemaker includes populations of two types of cells, called on-cells and off-cells (Fig. 4). On-cells inhibit off-cells, and off-cells inhibit on-cells. This property of mutual inhibition leads to the prediction that each suprachiasmatic nucelus contains populations of pacemaker opponent processes. In a model pacemaker that represents a diurnal mammal, light is assumed to excite on-cells. In a model pacemaker that represents a nocturnal mammal, light is assumed to excite off-cells. These hypotheses enable the model to explain both the complementary reactions to light of nocturnal and diurnal mammals and their similar phase response curves (PRC's) to pulses of light, as well as the PRC "dead zone" during the subjective day of a nocturnal mammal (Carpenter & Grossberg, 1983*b*; Pohl, 1982).

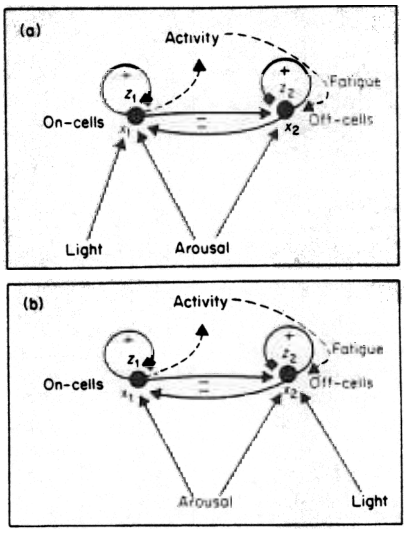

FIG. 4. Gated pacemaker circuits of diurnal (a) and nocturnal (b) models. In both circuits, on-cells and off-cells excite themselves via positive feedback, inhibit each other via negative feedback, and are tonically aroused. Light excites on-cells in the diurnal circuit and off-cells in the nocturnal circuit. Activation of on-cells or suppression of off-cells energizes wakefulness and activity. Fatigue builds up during the wakeful state and excites off-cells in both diurnal and nocturnal circuits. A conditionable slow gain control process activates on-cells in both diurnal and nocturnal circuits. Versions of the slow gain control process are shown in Figs 13, 16, and 18.

The hypothesis that both on-cells and off-cells form part of the SCN pacemaker is consistent with neurophysiological data showing that electrical stimulation of the optic nerve, or stimulation of the retina by light, excites some SCN cells while inhibiting other SCN cells (Groos, 1982; Groos & Hendricks, 1979; Groos & Mason, 1978; Lincoln, Church & Mason, 1975; Nishino, Koizumi & Brooks, 1976). These experiments unequivocally show that both on-cells and off-cells exist in the SCN by demonstrating that increments in light intensity cause increasing activity in some SCN cells and decreasing activity in other SCN cells. Complementing these studies of single cells, there are studies of multiple unit activity and of overall SCN metabolism using 2-deoxyglucose (Green & Gillette, 1982; Groos & Hendricks, 1982; Inouye & Kawamura, 1979; Sato & Kawamura, 1984; Schwartz & Gainer, 1977; Schwartz, Davidsen & Smith, 1980; Schwartz *et al.*, 1983; Shibata *et al.*, 1982). These studies show that a daytime peak in SCN activity can occur in both nocturanal and diurnal animals. There is little discussion in the literature concerning how the on-cell and off-cell

SCN cell populations contribute to the overall level of SCN metabolism. In fact, Groos & Mason (1980, p. 355) write: "It remains unclear why the SCN is equipped with two oppositely reacting visual subsystems, the light activated and the light suppressed cell types." Some 2-deoxyglucose results do point to an involvement of opponent responses in the SCN pacemaker. For example, Schwartz *et al.* (1980) show that 2-deoxyglucose utilization can be decreased by light input during certain phases of the SCN rhythm. They conclude that "measured levels of SCN glucose utilization do not translate simply into firing rates of SCN output cells; rather, they represent complex, weighted summations of myriad excitatory and inhibitory events within the nucleus" (p. 166).

Our model is consistent with both the data about SCN on-cells and off-cells and the data about daytime peaks in overall SCN activity if the following hypothesis is made: The population of SCN pacemaker cells which receives light inputs is larger, or has stronger output signals, than the population of pacemaker cells which does not receive light inputs, in both the diurnal and nocturnal mammals. This hypothesis is consistent with the data on on-cell and off-cell responses in the rat and the cat that Groos & Mason (1980) and Nishino *et al.* (1976) have reported. In both of these studies, light-activated cells were encountered approximately twice as often as light-suppressed cells. The hypothesis of more light-activated than light-suppressed cells reconciles single cell, multiple unit, and metabolic data as follows. In a diurnal gated pacemaker model, increased on-cell activity would dominate decreased off-cell activity during the subjective day, thereby causing a peak in overall SCN activity. In a nocturnal gated pacemaker model, increased off-cell activity would dominate decreased on-cell activity during the subjective day, thereby again causing a peak in overall SCN activity. Because the data have not yet fully determined how on-cells and off-cells contribute to SCN pacemaker dynamics, we have analysed the simplest *symmetric* gated pacemaker model in which the on-cell and off-cell populations have the same parameters. All of our arguments can be translated into the asymmetric case.

To clarify the relationship of on-cells and off-cells to multiple unit and metabolic indices of SCN activity, the following experiments would be very helpful:

(1) Continuously measure single unit SCN activity in DD. Observe whether each cell is day-active or night-active. Then use light inputs to test whether each cell is an on-cell or an off-cell. Count the number of cells encountered of each type.

(2) In LD, test whether the activity of some cells is in-phase with light whereas the activity of other cells is out-of-phase with light. The similarity

of SCN multiple unit activity in DD and LD (Sato & Kawamura, 1984) leads to the expectation that cells which are mutually out-of-phase in LD will also be out-of-phase in DD.

In a gated pacemaker model, until on-cells and off-cells are caused to differentially interact with processes external to the SCN, there is no distinction between a nocturnal and a diurnal pacemaker. Two feedback interactions with the SCN pacemaker are posited in the model: the output interaction whereby the pacemaker energizes observable behavior, and the input interaction whereby the fatigue signal homeostatically modulates pacemaker activity.

In both the nocturnal pacemaker and the diurnal pacemaker, behavior is energized when on-cells are active and off-cells are inactive. When the difference between on-cell activity and off-cell activity becomes sufficiently great, an output signal is generated from the pacemaker. A time-average of this output signal, taken on an ultradian time scale, determines the size of the fatigue signal. The fatigue signal is partly due to metabolic consequences of overt behavioral activities that are energized by the pacemaker output signal. Overt activity is not, however, the only metabolic source of fatigue. In particular, physical restraints imposed upon an awake experimental subject do not prevent a fatigue signal from feeding back to the pacemaker.

In both the nocturnal pacemaker and the diurnal pacemaker, the fatigue signal is assumed to excite off-cells, thereby indirectly inhibiting on-cells (Fig. 4). Thus both light and fatigue signals act at the off-cells of a nocturnal pacemaker, whereas light acts at the on-cells and fatigue acts at the off-cells of a diurnal pacemaker. This asymmetric action of light and fatigue across diurnal and nocturnal models has been used to explain the violation of Aschoff's rule (circadian period as a function of LL) by diurnal mammals but not nocturnal mammals, the consistent adherence to the circadian rule (behavioral activity as a function of LL) of both diurnal and nocturnal mammals, and the tendency of nocturnal mammals to lose circadian rhythmicity at lower light levels than diurnal mammals (Aschoff, 1979; Carpenter & Grossberg, 1984). The posited interaction between light and fatigue also leads to several predictions. For example, nocturnal mammals which obey Aschoff's rule will either be arrhythmic or violate Aschoff's rule if their fatigue signal is blocked before it can affect the SCN pacemaker; in nocturnal mammals, there are SCN pacemaker cells where the effects of a light pulse and the fatigue signal summate (Fig. 4(b)); in diurnal mammals, a light pulse and the fatigue signal are mutually inhibitory at all SCN pacemaker cells (Fig. 4(a)); in both diurnal and nocturnal mammals, a light pulse excites some SCN cells and inhibits other SCN cells.

The relationship between Aschoff's rule and split rhythms that our model posits can be used to suggest other predictions. For example, Pittendrigh & Daan (1976*b*, p. 336) review data which show that certain diurnal mammals split their rhythm when light intensity (LL) is increased whereas other diurnal mammals split their rhythm when light intensity is decreased. Our concept of the fatigue process relates this variability in the split rhythm data of diurnal mammals to the violations of Aschoff's rule in diurnal mammals (section 17). Nocturnal mammals, by contrast, tend to split their rhythm in response to light increases and also tend to consistently obey Aschoff's rule. In order to test more precise details about the relationship between split rhythm variability and Aschoff's rule violations, parametric data are needed that control for processes which are theoretically important. For example, self-selected light–dark cycles, dark nests, and lighting regimes that compensate for eye closure during sleep are all factors which influence predictions about Aschoff's rule (Carpenter & Grossberg, 1984).

Using this theoretical background, some of the factors that cause split rhythms in a nocturnal model can now be summarized. The presence of constant light (LL), when combined with a large fatigue signal, can prematurely induce sleep by causing abnormally rapid activation of the off-cells. In the model the total on-cell output determines the size of the fatigue signal that will be registered at the off-cells. Consequently, any procedure that reduces the total on-cell output can eliminate a split rhythm because the total on-cell output determines the size of the fatigue signal, and thus the total input to the off-cells. This explanation of how reducing total on-cell output can eliminate a split rhythm tacitly assumes that the fatigue signal is registered at all the off-cells in a nonspecific fashion (Carpenter & Grossberg, 1983*a*, 1984).

If one model SCN is removed, then the total on-cell output is greatly reduced. A split rhythm in the model can be abolished by such an ablation (Carpenter & Grossberg, 1982). Pickard & Turek (1982) have shown that surgical ablation of one SCN in the golden hamster does eliminate its split rhythm. They also recognized that this result may not be due to out-of-phase oscillators: "... the two SCN oscillators ... might normally be coupled, but this coupling might be altered under ... the split condition ... Another possibility is that a set of interacting pacemakers may reside in each SCN, and the loss of the split rhythm may be a consequence of the total number of these oscillators destroyed; whether or not the destruction is unilateral may not be important" (Pickard & Turek, 1982, p. 1121).

Our model also predicts that partial extirpation of both SCN can abolish splits by reducing total on-cell output. This prediction assumes that the

remaining SCN oscillating circuits and signal pathways are not damaged by the lesion.

Other investigators have suggested that split rhythms are caused when two populations of oscillators become out-of-phase (Daan & Berde, 1978; Gwinner, 1974; Hoffmann, 1971; Moore-Ede *et al.*, 1982; Pittendrigh, 1974). Many of these contributions use phenomenological or algebraic statements to describe how this occurs. Kawato & Suzuki (1980) have furthered this analysis by studying the parameters that control rhythm splitting in a dynamical model of coupled FitzHugh-Nagumo oscillators. The same qualitative conclusions can, however, be drawn using other classical oscillators, such as van der Pol oscillators. In such a model, the strength of the inhibitory coupling between the oscillators determines whether they will be driven out-of-phase. To explain split rhythms in both nocturnal and diurnal animals using light-sensitive inhibitory coupling strengths, one needs to suppose that light strengthens the inhibitory coupling between the oscillators of models that split in the light, and weakens the inhibitory coupling between the oscillators of models that split in the dark. The inhibitory coupling between oscillators also has to be weak to prevent splits in the dark, and strong to prevent splits in the light. In our model, by contrast, split rhythms

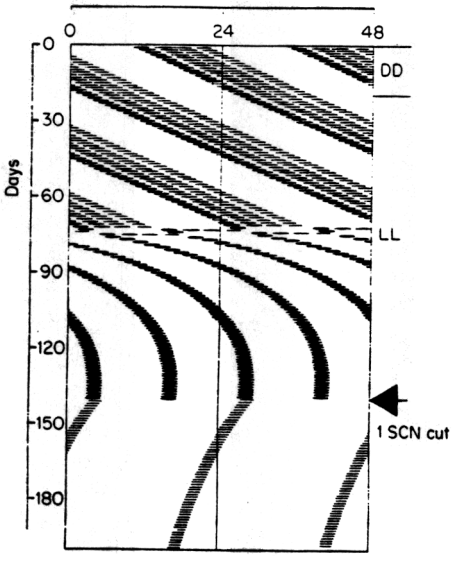

FIG. 5. A split rhythm and SCN ablation simulation: The text describes how the activity rhythm starts to split 52 days after being placed in steady light (LL) and how the split rhythm is abolished by ablation of one model SCN.

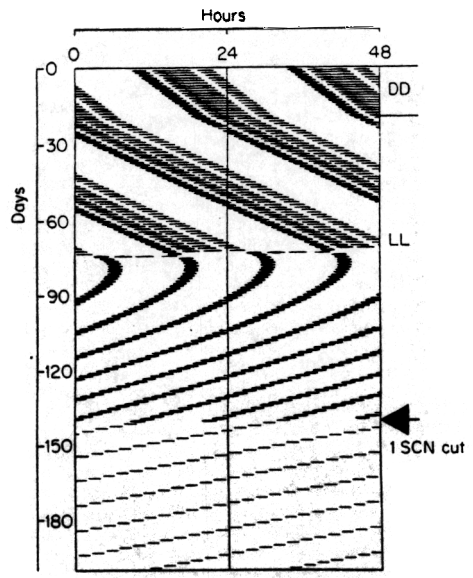

FIG. 6. A split rhythm and SCN ablation simulation: Simulation of the same experiment as in Fig. 5 using a related version of the model, to be described in section 10. Behavioral properties such as the duration of the transition from the non-split rhythm to the split rhythm can vary with model parameters. Gradual or abrupt transitions can occur both in the model and in behavioral data.

can occur when the homeostatic fatigue signal and the nonhomeostatic slow gain control process react to certain lighting regimes.

Figures 5 and 6 depict the model simulations of a split rhythm experiment and SCN ablation experiment of Pickard & Turek (1982) in which they study golden hamsters. The dark bars indicate the times at which the model animal is active. In Fig. 5, the model is kept in the dark (DD) for 20 days and then is placed in constant light (LL). Initially, the free-running period (τ) increases, as predicted by Aschoff's rule (Aschoff, 1960, 1979). On day 72, the rhythm starts to split. The split rhythm stabilizes after 5 days of transitional activity. The split period is shorter than the period prior to the split, as in the data. One model SCN is ablated on day 140, after which the split rhythm is abolished. The subsequent τ is shorter than any previous τ, as in the data.

Figure 6 shows that fine details of the split and its abolition can depend on model parameters. Carpenter (1983) describes yet another parametric choice in which, for example, the transitional period leading to the split is 15 days long, rather than 5 days long as in Fig. 5. Figure 7 shows that the

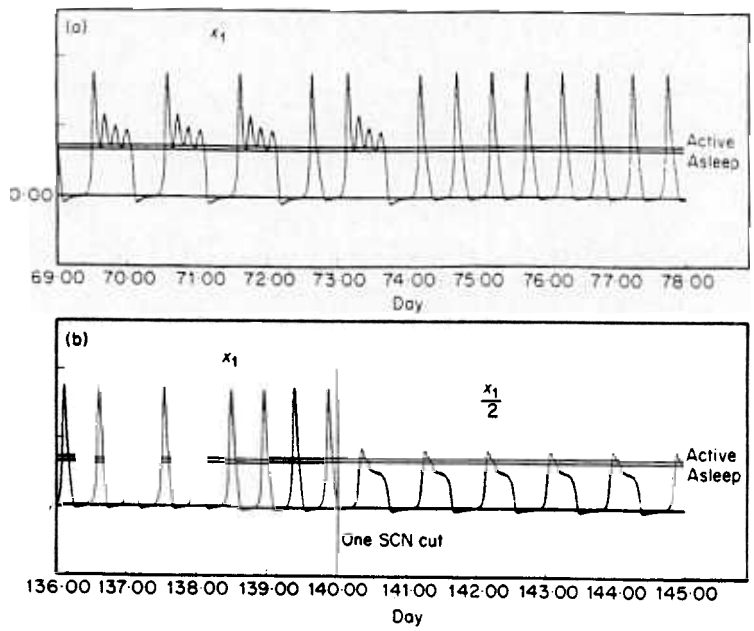

FIG. 7. Real-time plot of the pacemaker on-cell activity $x_1(t)$, defined in section 5. In (a), the multimodal activity waveform becomes unimodal after the split rhythm emerges. In (b), the split rhythm changes waveform when the split is abolished by ablation of one model SCN. Section 14 describes why $x_1(t)$ is plotted before the ablation and $\frac{1}{2}x_1(t)$ is plotted after the ablation.

wave form of on-cell activity through time is qualitatively different during different phases of the simulation. Figure 7 thus illustrates how a single oscillator circuit can generate very different wave forms. Figure 7(a) depicts the on-cell activity several days before and after the split occurs. Note the multimodal activity profile that exists before the split. Figure 7(b) depicts the on-cell activity before and after the ablation of one model SCN. Again the activity profile undergoes a qualitative change in form, amplitude, and period due to the transition. Throughout the time intervals depicted in Fig. 7, the light regime is constant (LL).

Earnest & Turek (1982) also perform split rhythm experiments in which hamsters are returned to DD for 10 to 30 days after having split their rhythm in LL. The return to DD eliminates the split rhythm. If animals are returned to LL 4–5 hours after their activity cycle begins, then the split rhythm is often promptly re-established. If animals are returned to LL at other phases of their circadian cycle, their split rhythm can reappear weeks later.

Earnest & Turek suggest that the rapid onset of splitting may be "due to the abrupt onset of light phase delaying one oscillator, while the other is phase advanced, which rapidly leads to the oscillators being 180° out-of-phase with each other" (p. 411). This hypothesis assumes that some oscillators only phase delay in response to light, other oscillators only phase advance in response to light, and the two types of oscillators are mutually inhibitory. The hypothesis is compatible with the experiment in question, but conceptual and mechanistic questions remain. For example, the splitting property reported by Earnest & Turek is clearly sensitive to both the onset of light and to its maintenance after onset. Were the property dependent only on light onset, splits should occur wherenever light pulses cause phase delays or advances 4–5 hours after the onset of activity. Were the property dependent only on light maintenace, animals should split independent of the activity phase during which a light is turned on and thereafter maintained. The suggested explanation of Earnest & Turek focusses upon the initiation of the split by a properly timed light onset. The further development of the split could then be discussed in terms of a light-sensitive, history-dependent inhibitory coupling strength between the two types of oscillators.

An alternative explanation of these data can be offered. Within our theoretical framework, transmitter gating actions have been hypothesized to occur in visual pathways (Carpenter & Grossberg, 1981) as well as in the pathways whereby other sensory cues, such as food and water cues, activate motivational hypothalamic circuits (Grossberg, 1975, 1982*a*, 1984*a*). These gating actions recalibrate the sensitivity, or adapt, input pathways in response to sustained cues, much as they recalibrate the sensitivity of a gated pacemaker's positive feedback loops, albeit on a different time scale. Let such a transmitter gating action modulate the light-activated input pathway to the pacemaker. Then an overshoot in input intensity occurs in response to light onset, followed by habituation of the input intensity to a lower level in response to sustained light. Suppose that this input overshoot occurs at a time when the fatigue feedback signal is large due to several hours of prior activity. Then the sum of the large light input plus the large fatigue signal may initiate a split if the slow gain process has not totally recovered from the prior split. By contrast, if the light input overshoot and the large fatigue feedback signal do not coincide, then a split will not occur until the slow gain control process can equilibrate to the input level due to the sustained light. Further experiments are needed to settle the issue.

The hypothesis that an input overshoot occurs at light onset does not imply that the mechanisms needed to explain parametric and nonparametric

after-effects are different (section 3). Indeed, both LL and LD lighting conditions are still functionally nonparametric at the pacemaker. In both cases, the input overshoot that may occur when an animal awakens or emerges from a dark nest does not coincide with a large fatigue signal.

5. The Gated Pacemaker Model

The gated pacemaker model describes the dynamics of on-cell/off-cell pairs, called *gated dipoles*, in which the on-cells and the off-cells mutually inhibit one another. Populations of these gated dipoles are assumed to exist in each SCN. The following processes define the gated pacemaker dynamics that are used in this article (Fig. 4).

1) Slowly accumulating transmitter substances are depleted, or habituated, by gating the release of feedback signals.

2) The feedback signals are organized as an on-center off-surround, or competitive, anatomy.

3) Both on-cells and off-cells are tonically aroused.

4) Light excites the on-cells of a diurnal model and the off-cells of a nocturnal model.

5) The on-cells drive observable activity, such as wheel-turning, in both the diurnal model and the nocturnal model.

6) On-cell activity gives rise to a fatigue signal that excites the off-cells in both the diurnal model and the nocturnal model. The fatigue signal is a time-average of the on-cell output signal on an ultradian time scale.

7) On-cell activity gives rise to a slowly varying gain control signal that excites the on-cells in both the diurnal model and the noctural model. The gain control signal is a time-average of the output signal on a time scale of months.

The general model equations for a nocturnal gated pacemaker are defined as follows.

NOCTURNAL MODEL

On-potential

$$\frac{dx_1}{dt} = -Ax_1 + (B - x_1)[I + f(x_1)z_1 + Sy] - (x_1 + C)g(x_2),$$

Off-potential

$$\frac{dx_2}{dt} = -Ax_2 + (B - x_2)[I + f(x_2)z_2 + F + J(t)] - (x_2 + C)g(x_1),$$

On-gate

$$\frac{dz_1}{dt} = D(E - z_1) - Hf(x_1)z_1, \tag{3}$$

Off-gate

$$\frac{dz_2}{dt} = D(E - z_2) - Hf(x_2)z_2, \tag{4}$$

Fatigue

$$\frac{dF}{dt} = -KF + h(x_1), \tag{5}$$

Gain control

$$\frac{dy}{dt} = -Uy + Vf(x_1). \tag{6}$$

Variable x_1 in equation (1n) is the potential of an on-cell (population) v_1. Variable x_2 in equation (2n) is the potential of an off-cell (population) v_2. Both x_1 and x_2 obey membrane equations (Hodgkin, 1964; Katz, 1966; Kuffler & Nicholls, 1976; Plonsey, 1969). In (1n) and (2n), the parameter $-A$ in the terms $-Ax_1$ and $-Ax_2$ determines the fast decay rate of the potentials x_1 and x_2. Also in (1n) and (2n), term I represents the constant arousal level that equally excites v_1 and v_2. In (1n), the transmitter substance z_1 gates the non-negative feedback signal $f(x_1)$ from v_1 to itself. Term $f(x_1)z_1$ is proportional to the rate at which transmitter is released from the feedback pathway from v_1 to itself, thereby re-exciting x_1. Term Sy describes the effect of the gain control process y on v_1 (Fig. 8). Term S is a signal that

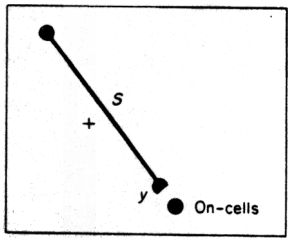

FIG. 8. The slow gain control process y gates the performance signal S. The gated signal Sy activates the on-cell potential x_1 and alters its rate of change. Choices of S and laws for the temporal evolution of y are described in sections 7, 9, and 11.

is gated by y, thereby generating a net excitatory input Sy at the on-cells v_1. The choice of signal S is described below, as well as its possible cellular realizations. The off-cells v_2 inhibit the on-cells v_1 via the non-negative signal $g(x_2)$ in term $-(x_1+C)g(x_2)$. Equation (2n) is the same as equation (1n), except that the indices 1 and 2 are interchanged; both the light input $J(t)$ and the fatigue signal F excite v_2 but not v_1; and the slow gain control process excites v_1 but not v_2.

Equations (3) and (4) define the transmitter processes z_1 and z_2. In equation (3), the transmitter z_1 accumulates to its maximal level E at a slow constant rate D via the term $D(E-z_1)$. This slow accumulation process provides a lumped description of a temperature compensated system of biochemical reactions. This slow accumulation process is balanced by the release of z_1 at rate $Hf(x_1)z_1$, leading to the excitation of x_1 in equation(1n). A similar combination of slow accumulation and gated release defines the dynamics of transmitter z_2 in equation (4).

The endogenous interactions between potentials x_1 and x_2 and transmitters z_1 and z_2 define a clock-like pacemaker (Carpenter & Grossberg, 1983*b*). This pacemaker has a stable period in the dark that varies inversely with the transmitter accumulation rate. Any genetic or prenatal factor capable of fixing this accumulation parameter can specify the period of the clock in the dark. The remaining processes F and y modulate the behavioral patterns that are generated by the pacemaker, as during split rhythms and long-term after-effects, but are not the source of the pacemaker's clock-like properties. Both F and y average indices of pacemaker activity, but are not independent oscillators.

The fatigue signal F in equation (5) is a time-average of $h(x_1)$, which increases with on-cell activity x_1. Speaking inuitively, an increase in x_1 and a decrease in x_2 arouse neural circuits that support the awake state. Fatigue builds up as a function of increased metabolic activity during the awake state, including but not restricted to overt action. Fatigue, in this sense, can thus build up in an alert but physically restrained animal. Since F excites the off-cells v_2 in equation (2n), it tends to inhibit the arousal generated by the pacemaker. The decay rate K of the fatigue signal F is assumed to be ultradian. In particular, $A > K > D$ so that the potentials x_1 and x_2 react faster than the fatigue signal F, which in turn reacts faster than the pacemaker gates z_1 and z_2.

The slow gain control process y in equation (6) is also a time-average, but on a time scale that is much slower than the circadian time scale. Process y averages term $Vf(x_1)$ at an averaging rate U. Then Sy in (1n) acts as an excitatory input to the on-cells v_1. Term Sy in equation (1n) combined with equation (6) formally define a long-term memory trace y (Grossberg, 1968,

1969, 1982*a*). In all the simulations, terms S, U, and V are chosen to be constant, or to vary as a function of light or on-cell activity. A single choice of these terms can be used, for example, to simulate all of the long-term after-effects. These choices are described in sections 7, 9 and 11.

The diurnal model differs from the nocturnal model only in the equations (1d) and (2d) that define its on-cell and off-cell potentials. In particular, light input $J(t)$ excites the on-cells but not the off-cells of the diurnal model. By contrast, the fatigue input F excites off-cells in both the diurnal and the nocturnal models, and the slow gain input y excites on-cells in both the diurnal and the nocturnal models. The diurnal model equations are listed below.

DIURNAL MODEL

On-potential

$$\frac{dx_1}{dt} = -Ax_1 + (B - x_1)[I + f(x_1)z_1 + J(t) + Sy] - (x_1 + C)g(x_2),$$

Off-potential

$$\frac{dx_2}{dt} = -Ax_2 + (B - x_2)[I + f(x_2)z_2 + F] - (x_2 + C)g(x_1),$$

On-gate

$$\frac{dz_1}{dt} = D(E - z_1) - Hf(x_1)z_1, \tag{3}$$

Off-gate

$$\frac{dz_2}{dt} = D(E - z_2) - Hf(x_2)z_2, \tag{4}$$

Fatigue

$$\frac{dF}{dt} = -KF + h(x_1), \tag{5}$$

Gain control

$$\frac{dy}{dt} = -Uy + Vf(x_1). \tag{6}$$

6. Signal Functions, Activity Thresholds, and Attentuation of Light Input During Sleep

The models in equations (1)-(6) are completely defined by a choice of the signal functions f, g, and h; the light input $J(t)$; the signals S, U, and V; and the parameters. In all the simulations, the signal functions $f(w)$ and $g(w)$ in equations (1)-(6) are chosen to be threshold-linear functions of activity w

$$f(w) = g(w) = \max(w, 0). \tag{7}$$

The signal function $h(w)$ in equation (5) is defined by

$$h(w) = M \max[f(w) - N, 0]. \tag{8}$$

The definition of $h(w)$ can be interpreted as follows. We assume that $f(x_1(t))$ is the output signal of the pacemaker. Behavioral activity is triggered when $f(x_1(t))$ exceeds the positive threshold N. We assume that the function $h(x_1(t))$ defined by equation (8) provides an index of behavioral activity. Since by equation (7), $f(w) = w$ when $w \geq 0$, we can simplify the definition of $h(w)$ in equation (8) to

$$h(w) = M \max(w - N, 0). \tag{9}$$

Equation (5) says that the fatigue signal F builds up at a rate proportional to behavioral activity $h(x_1(t))$. Activity ceases when $x_1(t) \leq N$. During such a time interval, fatigue decays at the ultradian rate K. Defining fatigue in this way enables us to provide a relatively simple description of the model. In more complex versions of the model (section 18), the pacemaker output modulates the arousal level of motivational circuits (e.g. for eating, drinking, sex, exploratory activity). This arousal level helps to determine the sensitivity of these circuits to external and internal cues which trigger incentive motivational signals that energize observable behaviors. The resultant behaviors have metabolic consequences that contribute to the fatigue signal. Metabolic sources other than overt activity may also contribute to the fatigue signal, for example during a time interval when an alert animal is physically restrained or a human subject is confined to bed. This additional complexity has not been needed to qualitatively explain after-effects and split rhythms.

In the circadian literature (Aschoff, 1960), the total period (τ) is broken up into the time (α) during which the animal engages in overt activity and the remaining rest time (ρ). In our model, the time α corresponds to the time when

$$x_1(t) > N, \tag{10}$$

since equation (10) holds when $h(x_1(t)) > 0$. In our analysis, we further

subdivide ρ into the sleep time and a transitional time of wakeful rest before, after, and possibly within the overt activity or sleep cycle. To mathematically distinguish these states, we assume that a sleep threshold P exists such that when

$$P < x_1(t) \leq N, \tag{11}$$

the model is in a state of wakeful rest. When

$$x_1(t) \leq P, \tag{12}$$

the model is in a state of sleep (Figs 3 & 7).

We operationally define sleep in terms of its effects on the pacemaker. The main effect is that eye closure (or entering a dark nest) can attenuate the light input to the pacemaker. Letting $L(t)$ be the light input that reaches the pacemaker when its "eyes" are open, we define the net light input in equations (1d) and (2n) to be

$$J(t) = \begin{cases} L(t) & \text{if } x_1(t) > P \\ \theta L(t) & \text{if } x_1(t) \leq P \end{cases} \tag{13}$$

Parameter θ is a light attenuation factor. A value of $\theta = 1$ means that no light attenuation occurs during sleep. A value of $\theta = 0$ means that complete light attenuation occurs during sleep, either due to eye closure, access to a dark nest, or a self-selected light-dark cycle. The fact that θ is not always zero is implied by the ability of light pulses to phase shift a mammal's circadian rhythm while the mammal is asleep (Carpenter & Grossberg, 1983*b*; Pohl, 1982). In our analysis of Achoff's rule, light attenuation during sleep contributes to violations of the rule by diurnal mammals but not by nocturnal mammals (Carpenter & Grossberg, 1984).

Our definitions of wakeful rest and sleep are chosen for simplicity. In species for which a separate temperature pacemaker helps to control sleep onset, a more complex definition is needed to discuss situations where in the SCN and temperature pacemakers become desynchronized (Czeisler *et al.*, 1980; Wever, 1979). Also, our definition of the fatigue feedback signal assumes that no fatigue accumulates during wakeful rest. The simulations thus make the approximations that the fatigue signal builds up much faster during overt activity than during wakeful rest, and that all the oscillators controlling sleep onset are approximately synchronized. In species which spend most of their waking hours actively exploring or consummating, the lack of fatigue build-up during wakeful rest causes no loss of generality. In other species, an obvious extension of the model would postulate a smaller rate of fatigue build-up during wakeful rest than during overt activity.

7. Long-term After-effects: Slow Gain Control and Associative Conditioning

The long-term after-effects in Figs 1(a) and 2 are both generated by a single choice of the slow gain control process described in equations (1) and (6). The same choice of the gain control process can be used to simulate experimental after-effects of LD 1:23, LD 18:6, LD 12:12, LL, LD 10:10, and LD 14:14 (Pittendrigh & Daan, 1976a). In this section, we will describe this gain control process, explain how it works, and display after-effect simulations. We have also found that these after-effects can be simulated by certain variations of this gain control process but not others. Thus the simulations identify a small number of possible physiological mechanisms. These variations and their after-effects will also be described (section 9).

In Figs 9–11, the model starts out with identical initial data and free-runs in the dark (DD) for 30 days before being exposed to different lighting regimes for 90 days. Then the model free-runs in the dark (DD) for 30 days. Using this procedure, we can systematically compare after-effects. Table 2 describes the free-running periods τ_{DD} in the dark after the lighting regime terminates. A comparison of LD 1:23 and LD 18:6 in Fig. 9 confirms the conclusion drawn from Fig. 1 that an increase of light in this situation causes a decrease in τ_{DD}. A comparison of LD 12:12 and LL in Fig. 10 confirms the conclusion drawn from Fig. 2 that an increase of light in this situation causes an increase of τ_{DD}. In the comparison of LD 10:10 and

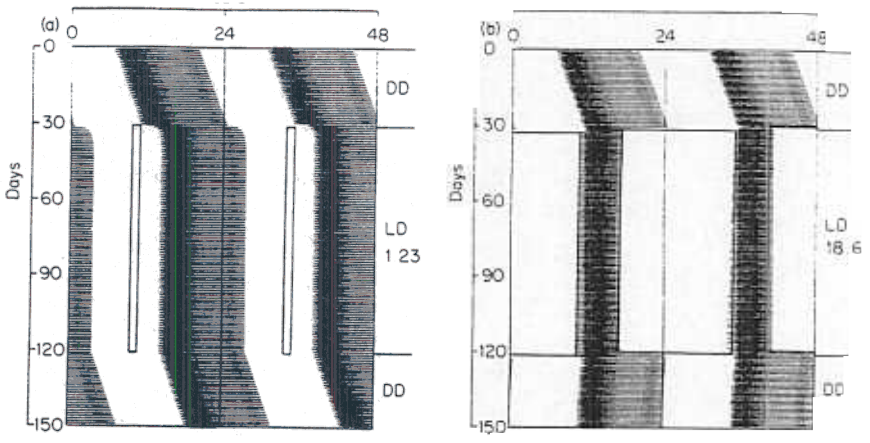

FIG. 9. Photoperiod after-effect simulations: Both simulations start with 30 days in the dark (DD), followed by a 90-day periodic light-dark (LD) lighting regime, followed by a 30-day free-run in the dark to test for after-effects. In (a), LD 1:23 is the lighting regime. In (b), LD 18:6 is the lighting regime.

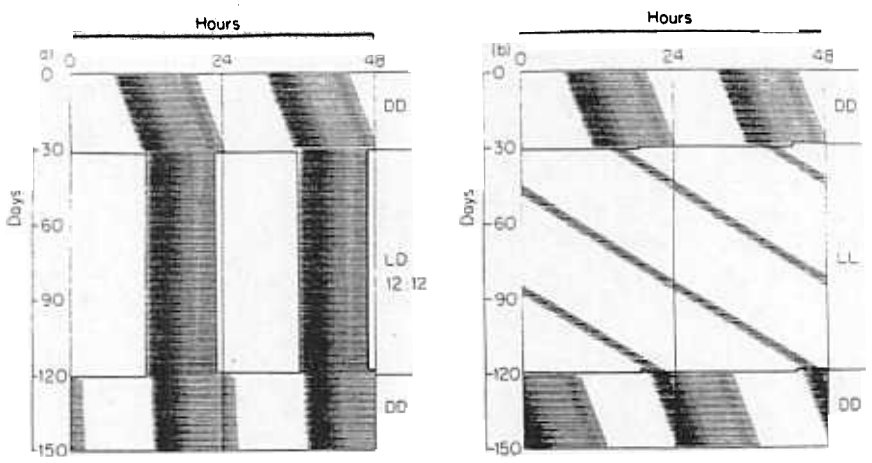

FIG. 10. After-effect of constant light: After-effects of an LD 12:12 lighting regime in (a) are compared with after-effects of an LL lighting regime in (b).

LD 14:14 in Fig. 11, the model is in the light one-half of the time in both simulations. As in the data of Pittendrigh & Daan (1976*a*), τ_{DD} is larger after LD 14:14 than after LD 10:10.

It cannot be overemphasized that the slow gain control process does not cause the circadian rhythmicity of the model pacemaker. The underlying

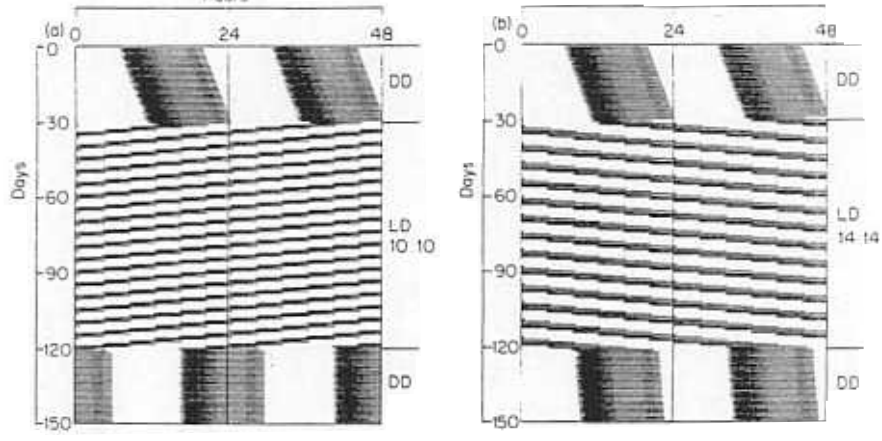

FIG. 11. After-effects of period: After-effects of an LD 10:10 lighting regime in (a) are compared with after-effects of an LD 14:14 lighting regime in (b). In both lighting regimes, light is on 50% of the time.

TABLE 2

	τ_{DD} after-effect (hours)	Figure
LD 1:23	24·15	9(a)
LD 18:6	23·97	9(b)
LD 12:12	24·01	10(a)
LL	24·15	10(b)
LD 10:10	23·99	11(a)
LD 14:14	24·04	11(b)

period of the pacemaker in the dark is controlled by the accumulation rate of the transmitter gates within the pacemaker's positive feedback loops (Fig. 4). It is precisely because of this endogenous rhythmicity that the fatigue signal and the slow gain control process are needed. The slow gain control process enables the pacemaker to adapt its activity cycles to long-term trends in the light-dark cycle. The fatigue signal exercises a homeostatic role that prevents the pacemaker from generating metabolically excessive bouts of activity. For example, the slow gain control process can enable a nocturnal model animal to become very active during the short nights of summer, while the fatigue feedback process prevents this heightened activity level from exhausting the model animal.

The slow gain control process is formally equivalent to a process of associative conditioning, and $y(t)$ in equations (1) and (6) obeys the law of a long-term memory (LTM) trace. In gated dipole models of appetitive hypothalamic circuits, a similar LTM process enables cues of various types to become conditioned reinforcers (Grossberg, 1972*b*, 1982*b*,*c*, 1984*a*). For example, cues that become conditioned reinforcers by being associated with food enable the eating circuit to adapt to temporally irregular presentations of food. Cues that become conditioned reinforcers by being associated with shock enable the fear circuit to anticipate expected occurrences of shock. A large data base about instrumental and classical conditioning of motivated behaviors leads to the conclusion that four conditionable pathways converge on an appetitive gated dipole circuit in response to each sensory cue capable of becoming a conditioned reinforcer for that circuit.

Our study of circadian after-effect data has guided us to choose versions of this LTM process specialized to deal with cues that are related to lighting conditions or activity levels. In every case treated so far, we have needed to invoke only one conditionable pathway, rather than four. Adding the other three pathways would not constitute a violation of principle, and future data may require this generalization.

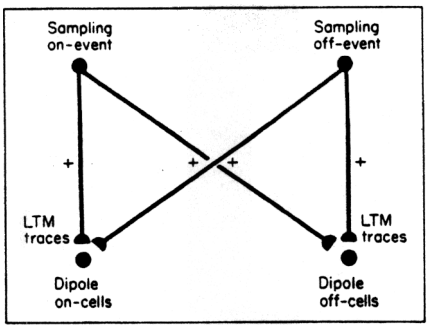

FIG. 12. In general, four conditionable pathways to the pacemaker may be influenced by a single sensory cue. Onset of the cue is an on-event that can cause performance signals to both the on-cells and the off-cells of a gated dipole circuit. Offset of the cue is an off-event that can also cause performance signals to both on-cells and off-cells. Each of these signal pathways can be gated by its own conditionable long-term memory (LTM) trace. All versions of our model that have been used in simulations employ only one of these four possible conditionable pathways.

A typical circuit in which four conditionable pathways modulate a gated dipole is depicted in Fig. 12. In Fig. 12, a cell population that is activated by an on-event sends sampling signals along a pair of conditionable pathways that abut the on-cells and the off-cells of the gated dipole. An LTM trace is computed at the end of each conditionable pathway. Each LTM trace gates the signals in its pathway before the gated signal can influence its target cells, as in Fig. 8. In Fig. 12, a cell population activated by an off-event can also send signals along a pair of conditionable pathways that abut the on-cells and the off-cells of the gated dipole. For example, an on-event population might be active whenever light is on, whereas an off-event population might be active whenever light is off. Increasing light intensity increases the activity of the on-event population and decreases the activity of the off-event population. Every event can hereby influence the activity of four conditionable pathways.

The after-effect experiments described in Section 3 can be explained using an LTM trace which temporally averages an index of on-cell activity while the model is awake. One version of this type of LTM trace is illustrated in Fig. 13. Each version is characterized by a special choice of S in equation (1) and of U and V in equation (6).

The LTM trace in Fig. 13 is the one that was used to generate Figs 1(a), 2, 3, 9, 10 and 11. This LTM trace gates a tonically active pathway. Hence the performance signal

$$S(t) \equiv S_{\text{tonic}}(t) = Q \tag{14}$$

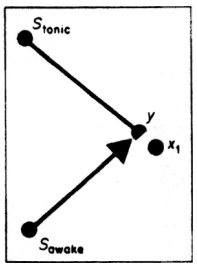

FIG. 13. A slow gain control process used in after-effect simulations: The LTM trace y time-averages x_1 when the model is awake and gates a tonically active performance signal, as in equations (14)-(19).

in equation (1), where Q is a positive constant. The terms U and V in equation (6) are both switched on when the model wakes up, and are switched off when the model goes to sleep. Thus

$$U(t) = RS_{\text{awake}}(t), \tag{15}$$

where R is a positive constant, and

$$V(t) = S_{\text{awake}}(t), \tag{16}$$

where

$$S_{\text{awake}}(t) = \begin{cases} 1 & \text{if } x_1(t) > P \\ 0 & \text{if } x_1(t) \leq P \end{cases} \tag{17}$$

Parameter P in equation (17) is the sleep threshold that was defined in equation (12). By equations (6), (15) and (16), equation (6) for the LTM trace is

$$\frac{d}{dt}y = S_{\text{awake}}[-Ry + f(x_1)].$$

By equation (17), S_{awake} is positive only when x_1 is positive. Since $f(x_1) = \max(x_1, 0)$ by equation (7), equation (18) can be written in the simpler form

$$\frac{d}{dt}y = S_{\text{awake}}[-Ry + x_1]. \tag{19}$$

By equation (19), the LTM trace $y(t)$ does not change when the model is asleep. When the model is awake, $y(t)$ averages the on-cell activity $x_1(t)$ at the rate R.

By equation (18), the sampling signal S_{awake} gates the sensitivity of y to the postsynaptic potential x_1. Process y is therefore located in Fig. 13

abutting synapses where it can both sample the postsynaptic potential x_1 and receive the presynaptic sampling signal S_{awake}.

8. Analysis of After-effects

In this section, we explain how the LTM trace $y(t)$, whose action is defined by equations (14) and (19), determines the experimentally correct periods in Figs 1(a), 2, 3, 9, 10 and 11. Figure 14 describes the critical

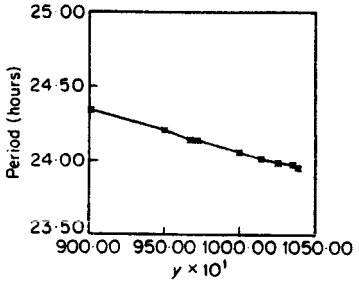

FIG. 14. Consistent after-effects on τ_{DD} depend upon a monotone decreasing relationship between the free-running period in the dark (τ_{DD}) and the size of the slow gain control variable (y).

property of this LTM trace. Figure 14 plots the model's period τ_{DD} during a free-run in the dark against the initial value of y at the onset of the free-run. The period τ_{DD} is a decreasing function of y. Thus if a previous lighting regime causes an increase in y, then the subsequent τ_{DD} will decrease, whereas if a previous lighting regime causes a decrease in y, then the subsequent τ_{DD} will increase.

Table 3 describes the effects of several lighting regimes on the size of y. Table 3 lists the value that y attains just before each lighting regime

TABLE 3

LD 1:23	$9{\cdot}7 \times 10^3$	9(a)
LD 18:6	$1{\cdot}0375 \times 10^4$	9(b)
LD 12:12	$1{\cdot}021 \times 10^4$	10(a)
LL	$9{\cdot}675 \times 10^3$	10(b)
LD 10:10	$1{\cdot}0285 \times 10^4$	11(a)
LD 14:14	$1{\cdot}01 \times 10^4$	11(b)

$S = Q$, $U = RS_{awake}$, $V = S_{awake}$

terminates. Using Fig. 14, these y values predict the τ_{DD} values during the subsequent free-run in the dark. This computation produces the τ_{DD} values that are listed in Table 2 and that are in accord with experimental data.

To understand these results, we need to explain how the lighting regimes in Table 3 cause their respective changes in y, and why τ_{DD} decreases as y increases. The first explanation requires an analysis of how the LTM equation (19) reacts to the lighting regimes. The second explanation requires an analysis of how different levels of y alter pacemaker dynamics via equation (1) for the on-cell potential x_1, in the case that the performance signal $S(t)$ is constant.

The main effect of different lighting regimes on y can be understood by comparing Figs 9(a) and 9(b), which describe after-effects of LD 1:23 and LD 18:6. During LD 1:23, on-cell activity is suppressed by light for only 1 hour every day. During LD 18:6, by contrast, on-cell activity is suppressed by light for 18 hours every day. Consequently, in the case of LD 18:6, on-cell activity is intense while the model is awake during the 6 hours of darkness. By contrast, in the case of LD 1:23, the model's activity, which is distributed over a larger period of time, is lower on the average.

The influence of the lighting regimes LD 12:12 and LL on y can be similarly understood. In particular, during LL the animal can only be active while light is suppressing its on-cells. Consequently the average on-cell activity while the animal is awake during LL is less than the average on-cell activity while the animal is awake during LD 12:12. Figure 10(b) illustrates the suppressive effect of LL on on-cell activity. The comparison of LD 10:10 with LD 14:14 makes a similar point. As in the comparison of LD 18:6 with LD 1:23, the on-cell activity cycle is compressed and intensified during LD 10:10 relative to LD 14:14. In summary, the single hypothesis that the LTM trace y averages on-cell potential while the model is awake suffices to explain the effects listed in Table 3 of both parametric and nonparametric lighting regimes on y.

It remains to explain how a parametric increase in y causes a decrease in τ_{DD}, as in Fig. 14. This property is due to the combined effects of the slow gain control and fatigue processes in our model. The model, in fact, predicts that systematic deviations from the observed after-effects will occur *in vivo* if the fatigue feedback signal is blocked. Predicted effects of blocking fatigue on Aschoff's rule are described in Carpenter & Grossberg (1984).

In the dark, equation (1) becomes

$$\frac{dx_1}{dt} = -Ax_1 + (B - x_1)[I + f(x_1)z_1 + Qy] - (x_1 + C)g(x_2) \qquad (20)$$

due to the assumption in equation (14) that $S(t)$ equals the constant Q. On

any given day, term Qy in equation (20) is approximately constant, since y is assumed to change very slowly. An increased value of y thus acts to enhance x_1 by a constant amount throughout the day. The primary effect of an increase in y is to approximately shift the graph of $x_1(t)$ upwards, as in Fig. 15. Such an approximate upward shift would cause a significant

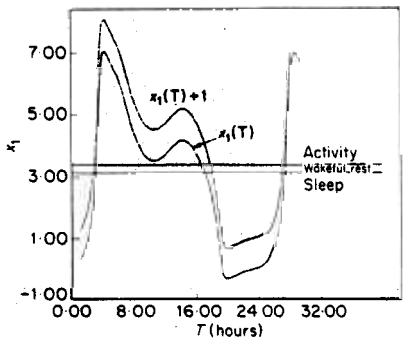

FIG. 15. An increase in the gain y tends to shift the graph of the on-cell potential x_1 upward. Such an upward shift tends to increase activity duration (α) and to decrease rest duration (ρ) without changing period (τ). In the figure, an upward shift of x_1 by 1 unit changes α from 13·51 hours to 14·85 hours and ρ from 10·64 hours to 9·30 hours. The period of both graphs is 24·15 hours.

increase in the duration of activity (α) and a significant decrease in the duration of rest (ρ) without significantly changing the period (τ). This primary effect of an increase in y is, however, modified by the action of the fatigue signal. The enhancement of activity due to an increase in y quickly generates a larger fatigue signal. This increased fatigue signal feeds back to the pacemaker. There it more actively excites the off-cells and thereby partially offsets the increased on-cell activity caused by the increased y. During sleep, on the other hand, fatigue decays to zero on an ultradian time scale. Fatigue is small long before the internal dynamics of the pacemaker wake the model up. The fatigue signal has a comparatively small effect on ρ. Thus an increase in y causes a relatively small increase in α, a relatively large decrease in ρ, and a net decrease in $\tau_{DD} = \alpha + \rho$, as in Fig. 14.

9. Alternative Slow Gain Control Processes

The discussion in section 8 explains the functional properties that enable an LTM process $y(t)$ to generate long-term after-effect data. The question therefore arises whether other LTM processes also possess these functional

properties. Two such LTM processes are described in this section. In these processes, light levels rather than activity levels determine the choice of S, U and V, and light acts as an off-event rather than as an on-event. These three examples of the LTM process, as a group, suggest the types of design variations that may be sought in physiological and biochemical data.

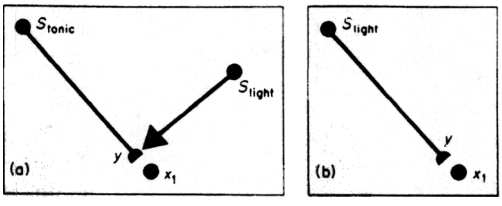

FIG. 16. Slow gain control processes used in after-effect simulations: In (a), the gain y averages on-cell output faster when light is off and slower when light is on, as in equations (23)-(24). The resultant gain y gates a tonically active performance signal, as in equation (14). In (b), both the rate of averaging by y and the size of the performance signal decrease when light is turned on, as in equations (23)-(25). Both (a) and (b) use the same conditioning rule for y.

Figure 16 described two light-sensitive LTM processes. In Fig. 16(a), the LTM trace gates a tonically active pathway. Hence the performance signal is

$$S(t) \equiv S_{\text{tonic}}(t) = Q \tag{14}$$

in equation (1), where Q is a positive constant. This is the same performance signal that was used in the previous LTM process. In the present case, however, the terms U and V in equation (6) are both inhibited when the light turns on, and are disinhibited when the light turns off. Thus

$$U(t) = RS_{\text{light}}(t) \tag{21}$$

and

$$V(t) = S_{\text{light}}(t),$$

where

$$S_{\text{light}}(t) = \frac{}{1 + WJ(t)} \tag{23}$$

and $J(t)$ is the light intensity defined by equation (13). By equations (6), (21) and (22), the equation for the LTM trace is

$$\frac{\mathrm{d}}{\mathrm{d}t}y = S_{\text{light}}[-Ry + f(x_1)]. \tag{24}$$

As in Fig. 13, the LTM trace gates a tonically active pathway. Unlike Fig. 13, the plasticity of the LTM trace is presynaptically gated by a pathway that is tonically on when light is off, but is inhibited when light turns on.

This LTM process has the requisite functional properties for the following reasons. The performance pathway that is gated by the LTM trace is tonically active, just as in the previous example. The presynaptic sampling signal S_{light} equals 1 in the dark and is approximately 0 in bright light. Since a nocturnal mammal tends to be active in the dark, S_{light} tends to be large when the animal is awake. Both sampling signals S_{light} and S_{awake} thus tend to be large during the same time intervals. The sampling signal S_{light} can also be large in the dark at times when the animal goes to sleep. This difference between S_{light} and S_{awake} can be used to devise lighting regimes capable of distinguishing which presynaptic sampling signal is operative in different animals. Table 4 lists the y values and τ_{DD} values that are generated by this version of the LTM process. All the τ_{DD} values are in the same direction as after-effect data.

TABLE 4

	τ_{DD} after-effects (hours)	
LD 1:23	23·47	$6{\cdot}55\times10^3$
LD 18:6	23·32	$7{\cdot}295\times10^3$
LD 12:12	23·28	$7{\cdot}67\times10^3$
LL	23·64	$5{\cdot}935\times10^3$
LD 10:10	23·28	$7{\cdot}65\times10^3$
LD 14:14	23·28	$7{\cdot}66\times10^3$

$S = Q$, $U = RS_{\text{light}}$, $V = S_{\text{light}}$

The third version of the LTM process also uses S_{light} to presynaptically gate the LTM sampling process. Consequently, equation (24) again holds. The performance signal is, however, no longer constant, as in equation (14). Instead, let

$$S(t) = QS_{\text{light}}(t). \tag{25}$$

Thus $S_{\text{light}}(t)$ is both the performance signal and the sampling signal in this process. Figure 16(b) shows that a separate presynaptic pathway is no longer needed to gate LTM sampling. A single pathway can accomplish both functions.

This LTM process has the necessary functional properties for the following reasons. Equation (24) for the LTM trace $y(t)$ is the same as in the previous model. The performance signal $S(t)$ in equation (25) equals the

constant Q in the dark. Except in the LL case, the performance signal tends to be constant when the animal is awake, as in the previous model. The performance signal decreases only at times when light excites the off-cells. The decrease in the performance signal $S(t)$ at the on-cells thus acts like an increase in light intensity $J(t)$ at the off-cells. Such a shift in the scale of light intensity does not damage the model's ability to simulate after-effects. Table 5 lists the y values and τ_{DD} values that are generated by this version of the LTM process. All the τ_{DD} values are in the same direction as after-effect data.

TABLE 5

	τ_{DD} after-effect (hours)	
LD 1:23	23·5	$6{\cdot}52 \times 10^3$
LD 18:6	23·4	$6{\cdot}835 \times 10^3$
LD 12:12	23·3	$7{\cdot}315 \times 10^3$
LL	23·9	$5{\cdot}4 \times 10^3$
LD 10:10	23·3	$7{\cdot}295 \times 10^3$
LD 14:14	23·3	$7{\cdot}29 \times 10^3$

$S = QS_{light}$, $U = RS_{light}$, $V = S_{light}$

10. Split Rhythms and Inconsistent After-effects on Period

The split rhythm simulations in Figs 5–7 are of data collected from the nocturnal hamster. The hamster does not, however, generate consistent after-effects on τ_{DD} (Pittendrigh & Daan, 1976*a*), despite the fact that it does exhibit after-effects and a slow onset of split rhythms. Thus one would not expect a model of hamster split rhythms to possess the same slow gain control process as a model which exhibits consistent after-effects on τ_{DD}.

The slow gain control processes which succeed in modelling split rhythm data do not, in fact, generate consistent after-effects on τ_{DD}. This is because, as a function of y, τ_{DD} is not monotone decreasing, as in Fig. 14. Instead, τ_{DD} varies nonmonotonically as a function of y, as in Fig. 17. Consequently, in one y range, τ_{DD} increases with y, whereas in a different y range, τ_{DD} decreases with y, thereby generating inconsistent after-effects on τ_{DD} across model animals.

It is also of importance, however, that the slow gain control processes which succeed in modelling split rhythm data are closely related to the processes that model consistent after-effects on τ_{DD}. Then one can envisage that a relatively simple evolutionary modification converts a model with

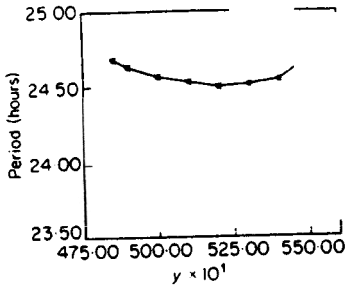

FIG. 17. Inconsistent after-effects on τ_{DD} occur when τ_{DD} depends in a non-monotonic way upon the size of y.

consistent after-effects on τ_{DD} to a model with split rhythms but inconsistent after-effects on τ_{DD}.

11. Split Rhythms: Slow Gain Control Processes

As in our discussion of after-effects, we will describe three variations of the slow gain control process that all possess the functional properties needed to generate split rhythm simulations. Then we will describe how these processes give rise to split rhythms, how they differ from processes that produce consistent after-effects on τ_{DD}, and how the graphs of τ_{DD} vs y in Figs 14 and 17 are related to data about Aschoff's rule (Aschoff, 1960, 1979).

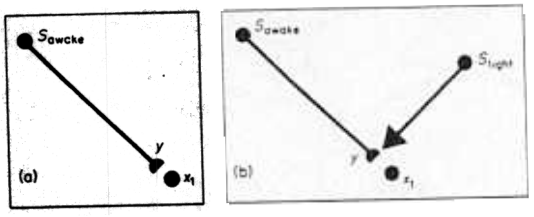

FIG. 18. Slow gain control processes used in split rhythm simulations: In all the processes, the performance signal is on only when the model is awake. The anatomy in (a) can support two closely related conditioning rules capable of causing split rhythms. In one rule, the gain y samples the on-cell output at a constant rate, as in equation (28). In the other rule, y samples the on-cell output only when the model is awake. In (b), the gain y samples on-cell output at a faster rate when light is off than when light is on.

Figure 18 depicts the anatomies of slow gain control processes that can give rise to split rhythms. In every case, the performance signal is the same; namely,

$$S(t) = QS_{awake}(t), \tag{26}$$

where

$$S_{\text{awake}}(t) = \begin{cases} 1 & \text{if } x_1(t) > P \\ 0 & \text{if } x_1(t) \leq P \end{cases} \tag{17}$$

In none of the models producing consistent after-effects on τ_{DD} was this performance signal used. The three split rhythm models use different U and V terms within the LTM trace equation (6). The functional property that all of these LTM traces guarantee is the following: y becomes smaller in LL than in DD.

The anatomy in Fig. 18(a) is the same for the first two models. In the first model,

$$\frac{d}{dt}y = -Ry + S_{\text{awake}} f(x_1);$$

that is, $U = R$ and $V = S_{\text{awake}}$. This LTM trace averages the product of S_{awake} and $f(x_1)$ at the constant rate R. The signal S_{awake} thus acts as a performance signal and a sampling signal. This model was used to generate Figs 6 and 7.

In the second model,

$$\frac{d}{dt}y = -Ry + f(x_1); \tag{28}$$

that is, $U = R$ and $V = 1$. This LTM trace averages $f(x_1)$ at the constant rate R.

The third model uses the anatomy in Fig 18(b). Its LTM trace is

$$\frac{d}{dt}y = S_{\text{light}}[-Ry + f(x_1)], \tag{29}$$

where

$$S_{\text{light}}(t) = \frac{1}{1 + WJ(t)},$$

and the light input $J(t)$ is defined by equation (13). Thus in equation (29), $U(t) = RS_{\text{light}}(t)$ and $V(t) = S_{\text{light}}(t)$. In this model, S_{awake} is the performance signal and S_{light} is the presynaptic sampling signal.

The split rhythm model in Fig. 18(b) differs from the after-effect model in Fig. 16(a) only in the choice of performance signal $S(t)$. Changing $S(t)$ from $S_{\text{tonic}}(t)$ to $S_{\text{awake}}(t)$ transforms the model from one capable of consistent after-effects on τ_{DD} to one capable of split rhythms and inconsistent after-effects on τ_{DD}.

12. Analysis of Split Rhythms: Depression of Gain by LL

All of the LTM traces in equations (27)-(29) have the property that y becomes smaller in LL than in DD for the following reasons.

By equation (2n), the light input $J(t)$ excites the off-cells during LL but not during DD. The off-cells, in turn, inhibit the on-cells due to equation (1n). Consequently, on the average, the on-cells are less active during LL than during DD. In equation (28), the LTM trace averages $f(x_1)$ at a constant rate R. Since x_1 is smaller, on the average, during LL than during DD, y becomes smaller during LL than during DD, as desired. Equation (27) differs from equation (28) only in that $f(x_1)$ is replaced by $S_{\text{awake}} f(x_1)$. Since S_{awake} equals 1 when the model is awake and equals 0 when the model is asleep, y averages $f(x_1)$ while the model is awake and averages 0 while the model is asleep. Since LL causes x_1 to be smaller on the average when the model is awake, y becomes smaller during LL than during DD, as desired.

In equation (29), $S_{\text{light}} \equiv 1$ during DD. Hence the LTM trace averages $f(x_1)$ at the constant rate R. During LL,

$$S_{\text{light}}(t) = \begin{cases} \dfrac{1}{1 + WL(t)} & \text{if } x_1(t) > P \\ 1 + W\theta L(t) & \text{if } x_1(t) \leq P \end{cases} \tag{30}$$

by equations (13) and (23). In equation (30), the light intensity $L(t)$ is a positive constant during LL. Since $\theta < 1$, $S_{\text{light}}(t)$ is larger when the model is asleep than when the model is awake. Consequently, the LTM trace averages the small x_1 values that occur during sleep faster than the larger x_1 values that occur during wakefulness. Moreover, during LL, all x_1 values are depressed on the average as compared to DD. Consequently, y becomes smaller during LL than during DD.

It remains to explain how the decrease of y during LL and the choice of performance signal $S = QS_{\text{awake}}$ in equation (26) generate split rhythms.

13. Analysis of Split Rhythms: Interaction of Slow Gain, Pacemaker Gate, and Fatigue

Our explanation of the slow onset of split rhythms is based upon properties of the interaction between the LTM trace, the fatigue signal, and the pacemaker. This explanation depends, moreover, on the fact that the pacemaker rhythm derives from an interaction between fast potentials and slow transmitter gates, as in equations (1)-(4) and Fig. 4. Thus the type of

explanation that we offer lies outside the scope of classical oscillator models, such as models based upon van der Pol oscillators.

The fatigue signal acts on an ultradian time scale in our model. Since an increase in model activity causes an increased build-up of fatigue, multimodal bouts of activity can be generated by the negative feedback that fatigue exerts upon the on-cells (Fig. 4). Such multimodal bouts of activity are visible on days 1-72 in Fig. 6, prior to the onset of the split rhythm.

The fatigue feedback acts on an ultradian time scale, whereas the transmitter gates act on a circadian time scale. Thus fatigue can build up before the on-cell transmitter gate in equation (3) become depleted. Model activity can thus be depressed by fatigue at times when on-cell transmitter gates are still quite large.

When the model is placed from DD into LL, its on-cell activity is depressed, on the average. Consequently, due to the form of the LTM trace equations (27), (28), or (29), y gradually decreases. As y gradually decreases, so too does its excitatory effect on the on-cell activity x_1 in equation (1n). The net effect of this feedback exchange between x_1 and y is a slow, progressive decrease in the average activity of x_1 while the LL lighting regime is maintained. Eventually a level of x_1 activity is approached at which an interaction between the performance signal $S(t) = QS_{\text{awake}}(t)$, the fatigue signal $F(t)$, and the transmitter gate $z_1(t)$ can initiate a split rhythm. How this happens can be understood by considering Fig. 7(a).

Figure 7(a) describes the on-cell activity $x_1(t)$ at times just before and just after the split rhythm is initiated. Note the multimodal activity bouts on days 70-72. On day 73, the first peak in activity is not followed by three subsequent peaks. This is because the LTM trace $y(t)$ has decreased to such a level that $x_1(t)$ falls below the sleep threshold P after the first peak. As soon as the model falls asleep, the performance signal $S(t) = QS_{\text{awake}}(t)$ in equation (26) suddenly becomes zero. Consequently the gain term $S(t)y$ in equation (1n) suddenly becomes zero. In effect, the on-cell activity loses a source of excitatory input at that moment. Due to this event, $x_1(t)$ continues to decrease after the model falls asleep, thereby preventing a multimodal activity bout from occurring.

At the time when this first bout of activity terminates, the on-cell transmitter gate $z_1(t)$ is relatively large. The fatigue signal, not the endogenous pacemaker rhythm, caused the onset of sleep. After sleep begins, the transmitter $z_1(t)$ grows to even larger values, while the fatigue signal $F(t)$ decays on an ultradian time scale. The combination of the decay of $F(t)$ and the large values of $z_1(t)$ wakes up the model after a relatively short sleep interval. As in Fig. 7(a), the multimodal activity bout may temporarily recover after the first unimodal peak is over. This transitional

time may last for a number of cycles that varies with the choice of model parameters. However, once $y(t)$ decreases a little more, a split rhythm is maintained by the interaction between fatigue $F(t)$, the on-cell transmitter gate $z_1(t)$, and the performance signal $S(t)$.

14. Analysis of Split Rhythms: SCN Ablation Experiments

In Fig. 6, on day 140, one model SCN is removed and the split rhythm is abolished. This effect was discovered by Pickard & Turek (1982) using hamsters. As we indicated in section 4, our model generates this effect due to the sudden decrease in fatigue feedback that is sensed by each surviving off-cell. This decrease is caused as follows.

Cutting out half of the model cells causes a sudden decrease in total on-cell output. The total fatigue signal is correspondingly reduced. Every surviving off-cell is influenced by the total fatigue signal. In other words, the output signals from all the on-cells combine to generate behavioral activity and fatigue. The fatigue level, in turn, is communicated non-specifically to every off-cell. This non-specific property of the fatigue signal is compatible with the hypothesis that fatigue feedback is delivered *in vivo* to SCN off-cells via the bloodstream.

Figure 7(b) plots the total on-cell potential of the model just before and after the ablation. Cutting out half of the on-cells reduces the size of the fatigue signal and thereby unmasks the basic unsplit pacemaker period. This basic pacemaker period is shorter than the pre-split pacemaker period, where fatigue prolongs the period by causing intermittent rest intervals during which $z_1(t)$ can recover.

Simulation of an SCN ablation is achieved by reducing the size of the on-cell output signal feedback to the pacemaker in equation (5). When half of the model SCN is removed, the feedback signal is reduced to half its previous size. Equation (5) then becomes

$$\frac{dF}{dt} = -KF + h(x_1/2). \tag{31}$$

This change is interpreted as follows. Equation (1) described the dynamics of a single on-cell potential x_1. Previously our model has considered situations in which all the on-cell potentials of the pacemaker are synchronized. Then x_1 is proportional to the sum of all the on-cell potentials in the pacemaker. By suitably interpreting the parameters that define $h(w)$ in equation (9), $h(x_1)$ in equation (5) can be defined as the total effect of all pacemaker cells on the fatigue signal. Cutting out half of the pacemaker cells reduces this total effect to $h(x_1/2)$, as in equation (31).

The graph in Fig. 7(b) describes $x_1(t)$ before the ablation and $\frac{1}{2}x_1(t)$ after the ablation. These functions are proportional to the sum of all pacemaker on-cell outputs before and after the ablation, respectively.

The significant reduction in total pacemaker activity after the ablation is also found in the Pickard & Turek (1982) data.

15. Fatigue as an Internal Zeitgeber

Another important effect of SCN ablation occurs in the Pickard & Turek (1982) data. After ablation, behavioral activity is reduced in both overall intensity and synchrony. The low levels of activity gradually become more diffusely distributed throughout each day.

In our model, both light and fatigue can act to synchronize the many on-cell off-cell dipoles that constitute the total pacemaker. In steady light (LL) or dark (DD), light loses it capacity to act as an effective external Zeitgeber. This is not, however, true of the fatigue signal, which can act as an internal Zeitgeber which is non-specifically sensed by all the off-cells.

After ablating half of the pacemaker cells, however, the fatigue signal is markedly reduced. Its ability to entrain the individual dipoles of the pacemaker is correspondingly reduced, so that these dipoles can gradually drift out-of-phase with one another.

16. Analysis of Inconsistent After-Effects on Period

It remains to analyse how a parametric increase in y causes a non-monotonic change in τ_{DD}, as in Fig. 17. This property is due to the combined effects of the slow gain control and fatigue processes in our model. The non-monotonic graph in Fig. 17 differs from the monotone decreasing graph in Fig. 14 due to a different choice of performance signal $S(t)$ in the corresponding models. The monotone decreasing graph of Fig. 14 was explained in section 8 using the tonically active performance signal

$$S(t) \equiv S_{\text{tonic}}(t) = Q. \tag{14}$$

The non-monotonic graph in Fig. 17 is due to the performance signal

$$S(t) = QS_{\text{awake}}(t) \tag{26}$$

where $S_{\text{awake}}(t)$ is defined by equation (17).

On any given day, the gain term y is approximately constant due to its slow rate of change. Thus the gated performance signal Sy in equation (1) changes significantly on any given day only if S changes. In section 8, we noted that Sy does not change significantly on any given day if $S(t) = S_{\text{tonic}}$,

as in equation (14). This is no longer true if $S(t) = QS_{\text{awake}}(t)$. Then by equations (17) and (26),

$$Sy = \begin{cases} Qy & \text{if } x_1 > P \\ 0 & \text{if } x_1 \leq P \end{cases} \tag{32}$$

By equation (32), Sy is the same for both the choices $S = S_{\text{tonic}} = Q$ and $S = QS_{\text{awake}}$ when the model is awake. Hence a parametric increase in y causes only a slight increase in α, by the same argument as in Section 8. By contrast with the case treated in Section 8, equation (32) implies that different values of y have no direct effect on the pacemaker during sleep. Thus other things being equal, increasing the value of y should have little effect on ρ. Since both α and ρ tend to change by only small amounts as y is increased, the net effect of these changes upon $\tau = \alpha + \rho$ can be an increase or a decrease in period, as illustrated by Fig. 17. A precise understanding of this situation requires a lengthy analysis. Such an analysis is provided for a formally identical problem concerning Aschoff's rule in Carpenter & Grossberg (1984). The formal relationship between this problem and Aschoff's rule is described in section 17.

Although an increase in LL causes a decrease in y (section 12), a decrease in y can cause a decrease or an increase in τ_{DD}. Thus an increase in LL does not cause consistent after-effects on τ_{DD} in a model animal capable of split rhythms.

We now describe a remarkable formal relationship between after-effects and Aschoff's rule. Parametric properties of Aschoff's rule have been extensively analysed in Carpenter & Grossberg (1984). This formal connection enables the Aschoff's rule analysis to be used to explain parametric properties of after-effects.

17. A Formal Connection Between After-effects and Aschoff's Rule

In its classical form (Aschoff, 1960), Aschoff's rule states that circadian period (τ) is an increasing function of LL in nocturnal animals and a decreasing function of LL in diurnal animals. The related circadian rule states that circadian activity (α) is a decreasing function of LL in nocturnal animals and an increasing function of LL in diurnal animals. The circadian rule has been upheld by many experiments on nocturnal mammals and diurnal mammals. By contrast, although Aschoff's rule consistently holds in nocturnal mammals, many exceptions to the rule have been observed in diurnal mammals (Aschoff, 1979).

These experimental properties also arise in gated pacemaker models of diurnal and nocturnal circadian rhythms (Carpenter & Grossberg, 1984).

The properties are due to the fact that light excites on-cells of a diurnal pacemaker and off-cells of a nocturnal pacemaker, whereas the fatigue signal excites off-cells in both diurnal and nocturnal pacemakers. The action of fatigue feedback is, in fact, necessary to explain Aschoff's rule in both diurnal and nocturnal pacemakers. An analysis of the interaction between fatigue feedback and the attenuation of light that occurs at the pacemaker during sleep explains both the Aschoff's rule and the circadian rule data. Several behavioral and physiological predictions aimed at testing this explanation are provided in Carpenter & Grossberg (1984), along with analyses of related data.

The formal connection between after-effects and Aschoff's rule can be seen by considering equation (1d) for the on-cell potential x_1 of a diurnal model. Consider term

$$Sy + J \tag{33}$$

in that equation. By equation (13), (33) can be written as

$$Sy + \Theta L, \tag{34}$$

where $L(t)$ is the external light intensity at time t, and

$$\Theta(t) = \begin{cases} 1 & \text{if model is awake} \\ \theta & \text{if model is asleep} \end{cases} \tag{35}$$

Recall that θ $(0 \leq \theta \leq 1)$ measures the amount of light attenuation at the pacemaker during sleep.

In a constant light condition (LL) and over a time span of a day, both y and L in equation (34) are approximately constant. This fact draws attention to a formal relationship between S and Θ (Table 6). If $\theta = 1$ in equation (35), then $\Theta \equiv$ constant. Similarly, the choice $S = S_{\text{tonic}}$ implies $S \equiv$ constant. If $\theta = 0$ in equation (35), then $\Theta = 1$ or 0 depending upon whether the model is awake or asleep. The same is true of S_{awake} in equation (17). Thus Sy influences after-effects on period in a nocturnal model in a manner formally identical to the effect of ΘL on period in a diurnal model exposed to LL.

TABLE 6

After-effects on τ_{DD}	Performance signal	Degree of light attenuation	Aschoff's rule in diurnal pacemaker
consistent	$S = Q$	$\theta = 1$	consistent
inconsistent	$S = QS_{\text{awake}}$	$\theta = 0$	inconsistent

Due to this correspondence, one expects that the choice $\Theta \equiv 1$ will generate a monotone decreasing dependence of τ on LL in an Aschoff's rule simulation. This graph is shown in Fig. 19(a). One also expects that choosing $\Theta = 1$ if the model is awake, and 0 if the model is asleep will generate a non-monotonic dependence of τ on LL in an Aschoff's rule simulation. This graph is shown in Fig. 19(b). This formal correspondence permits the quantitative analysis of Aschoff's rule and its exceptions in Carpenter & Grossberg (1984) to be used to explain consistent and inconsistent after-effects on τ_{DD}.

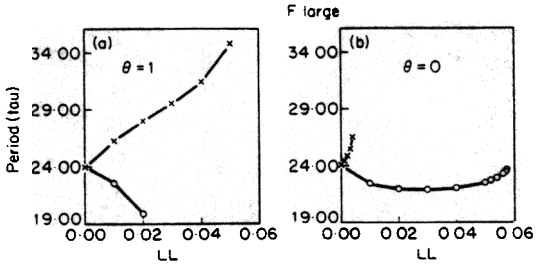

FIG. 19. Dependence of Aschoff's rule on light attenuation during sleep: In (a), no light attenuation occurs ($\theta = 1$). Period (τ) decreases as steady light intensity (LL) increases in the diurnal model; that is, Aschoff's rule holds. In (b), total light attenuation occurs ($\theta = 0$). Period (τ) is a non-monotonic function of steady light intensity (LL) in the diurnal model (○); that is, Aschoff's rule is violated. In the nocturnal model (×), Aschoff's rule holds whether or not light attenuation occurs.

18. Regulation of Motivated Behavior by Hierarchical Networks: The Homology Between Pacemaker Circuits and Motivational Circuits

Our conception of how pacemaker output modulates motivated behavior is outlined below. This conception joins together properties of the gated pacemaker with properties of neural network models that have been used to explain behavioral, evoked potential, physiological, and pharmacological data concerning reinforcement, drive, motivation, and attention (Grossberg, 1982*b*,*c*, 1984*a*). It also clarifies the sense in which gated pacemaker circuits are formally homologus to motivational gated dipole circuits. We hypothesize that both types of hypothalamic circuits *in vivo* are fashioned out of similar components, albeit in evolutionarily specialized designs.

Figure 20 describes a neural network that has been used to analyse data about motivated behavior. In Fig. 20, pathways such as 1 and 2 carry specific, but complementary, drive inputs (e.g. hunger vs satiety) to a single gated dipole circuit. Pathways labelled 3 carry non-specific arousal to this, and

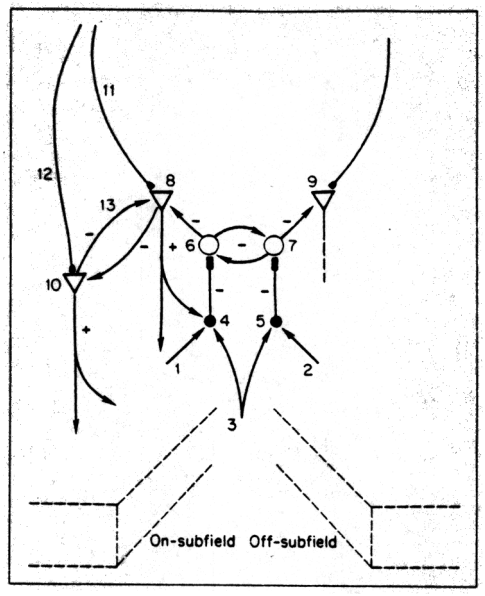

FIG. 20. A motivational dipole field: The text describes how individual motivational dipoles are joined together by competitive feedback networks to decide which dipole(s) will reverberate in short-term memory (STM) and thereby release positive or negative incentive motivation in response to the changing balance of reinforcing cue and internal drive signals. The gated pacemaker modulates the sensitivity of this motivational circuit by altering its arousal level (pathway 3).

every, motivational dipole in the network. We hypothesize that the gated pacemaker output modulates the size of the non-specific arousal input carried by pathway 3. This modulatory action will be described in detail below. In order to clarify how such an action can influence motivated behavior, it is first necessary to describe some of the basic properties of the network in Fig. 20.

Cells such as 4 and 5 add up their drive input (pathway 1 or 2) and arousal input (pathway 3) and thereupon inhibit the tonically active cells 6 and 7. (Tonic cells have open symbols; phasic cells have closed symbols.) Pathways $4 \rightarrow 6$ and $5 \rightarrow 7$ contain slowly accumulating transmitter gates (square synapses) that are assumed to be catecholaminergic. If drive input 1 exceeds drive input 2, then the transmitter in pathway $4 \rightarrow 6$ is depleted, or habituated, more than the transmitter in pathway $5 \rightarrow 7$. This differential habituation across the competing dipole channels calibrates the dipole for a possible rapid reset, or rebound event, later on.

Before input 1 exceeds input 2, the tonic cells 6 and 7 equally inhibit each other. As soon as input 1 exceeds input 2, cell 6 is inhibited more than cell 7. This imbalance disinhibits tonic cell 8 and further inhibits tonic cell 9. Both cells 8 and 9 are polyvalent, meaning that all their excitatory inputs must be active for these cells to vigorously fire. (Triangles denote polyvalence.) The polyvalent cells are assumed to be pyramidal cells. Because cells 8 and 9 are polyvalent, a larger input to cell 1 than cell 2 is insufficient to fire these cells. However, such an imbalance can prevent cell 9 from firing.

To see how cell 8 can fire, we consider the polyvalent cells, 8 and 10, of two different motivational channels (e.g. hunger vs sex). Cells 8 and 10 compete via the inhibitory pathways 13. The polyvalent cells 8 and 10 also receive inputs from external cue representations via the conditionable pathways 11 and 12, respectively. The long-term memory (LTM) traces of these pathways are computed within the filled hemicircles abutting cells 8 and 10. These LTM traces encode the conditioned reinforcing properties of their respective external cues. For example, a sensory cue that effectively predicts the occurrence of food will have large LTM traces abutting the hunger dipole's polyvalent on-cell population. The LTM traces are assumed to be cholinergic *in vivo* (Grossberg, 1972*b*).

The conditioned reinforcer inputs combine with drive and arousal inputs at their respective polyvalent cells, which begin to fire if their thresholds are exceeded. The polyvalent cells thereupon compete among themselves via the inter-dipole inhibitory interneurons 13, as they simultaneously try to excite themselves via positive feedback pathways such as $8 \rightarrow 4 \rightarrow 6 \rightarrow 8$.

If, say, cell 8 wins this competition, then its dipole generates incentive motivational output signals that can energize motivationally compatible action patterns. Simultaneously, the transmitter gate in pathway $4 \rightarrow 6$ is depleted, or habituated, due to the suprathreshold reverberation bursting through cell 8 via pathway $8 \rightarrow 4 \rightarrow 6 \rightarrow 8$. This reverberation simultaneously causes LTM changes in pathway 11. The reverberation hereby induced conditioned reinforcer changes in its abutting LTM traces even as it prepares the network, via the depleting transmitters, for motivational reset due to subsequent offset of the sensory cues controlling pathway 11.

The conditioned reinforcer pathways 11 and 12 in Fig. 20 are formally homologous to the slow gain control pathways in Figs 8 and 12. The satiety input pathway 2 in Fig. 20 is homologous to the fatigue feedback pathway in Fig. 4. Unconditional reinforcing inputs, such as taste or shock inputs (not pictured in Fig. 20), are homologous to the light input in Fig. 4. The on-cell and off-cell transmitter gates in pathways $4 \rightarrow 6$ and $5 \rightarrow 7$ of Fig. 20 are homologous to the on-cell and off-cell transmitter gates in Fig. 4. In Fig. 20, these transmitter gates occur within the positive feedback pathways

$4 \rightarrow 6 \rightarrow 8 \rightarrow 4$ and $5 \rightarrow 7 \rightarrow 9 \rightarrow 5$. In Fig. 4, the gates occur within positive feedback pathways $v_1 \rightarrow v_1$ and $v_2 \rightarrow v_2$. In Fig. 20, dipole competititon occurs between cell populations 6 and 7. In Fig. 4, dipole competition occurs between v_1 and v_2. Thus, although the gated dipoles in Figs 4 and 20 have been specialized to generate different functional properties, the formal homology that exists between the gated dipoles enables them to be recognized as variations on a common evolutionary design.

19. Circadian Modulation of Sensitivity: Inverted U in Motivational Dipoles

The circuitry in Fig. 20 determines which behavioral commands will incentive motivational signals through time. The pacemaker modulates how sensitively this circuit responds to its external reinforcer and internal drive inputs, and thus the circuit's ability to energize motivated behavior. The ability of pacemaker output to modulate motivational processing follows from a basic property of gated dipole circuits (Grossberg, 1972*b*, 1981*a*, 1984*a*,*b*). When a gated dipole's arousal level (pathway 3) is parametrically increased, the outputs of the dipole are altered according to an inverted U law: dipole outputs are depressed in response to input signals if the arousal level is chosen either too low or too high. The dipole optimally responds to phasic inputs at intermediate arousal levels.

We hypothesize that the pacemaker causes a circadian oscillation to occur in the arousal level of motivational circuits. The inverted U property of the gated dipoles in motivational circuits prevents these dipoles from reacting when their arousal level is too high or too low. Behaviors that require motivational signals for their execution will thus not be emitted if the circadian output is too high or too low (Grossberg, 1972*b*, 1981*a*, 1982*c*, 1984*a*). We hypothesize that, under normal conditions, the arousal level during the wakeful state brings motivational dipoles into the middle range of their inverted U.

It remains to discuss whether the arousal level becomes smaller ("underarousal") or larger ("overarousal") during sleep that it is during the wakeful state. We hypothesize that underarousal occurs during sleep. This hypothesis is based upon the following property of gated dipoles in the underaroused state. During underarousal, the threshold intensity that an input must exceed to generate an output signal is significantly raised. The network will not react to many inputs that would cause a reaction during the wakeful state. If, however, an input is sufficiently intense to exceed this elevated threshold, then the dipole output is hypersensitive to the input; that is, suprathreshold increments in the input cause larger than normal increments in dipole

output. Thus a dipole that is underaroused during sleep can react to intense inputs. An overaroused dipole, by contrast, does not react to inputs of any intensity.

Gated dipoles have been hypothesized to occur in circuits that carry out perceptual and cognitive processing (Grossberg, 1978, 1980, 1984*a*,*c*). Circadian oscillation of the non-specific arousal signal to these circuits can also modulate their sensitivity during the wake-sleep cycle.

20. The Underaroused and Overaroused Depressive Syndromes

From the perspective of the circadian wake-sleep cycle, the inverted *U* property of a gated dipole is a valuable one. This property also creates the danger that the arousal level may be improperly chosen during the wakeful state. Symptoms of mental disorders have been interpreted, and indeed predicted, using the formal syndromes of functional properties that obtain in underaroused and overaroused gated dipoles. These disorders include juvenile hyperactivity, Parkinsonism, hypothalamic hyperphagia, and simple schizophrenia (Grossberg, 1972*b*, 1984*a*,*b*). An unsolved problem of fundamental importance is to determine how the circadian pacemaker is calibrated to select an arousal level in the normal range during the wakeful state.

The hypothesis that motivational circuits are underaroused during sleep can be experimentally tested. For example, gated dipole dynamics predict the existence of a transitional period just before and/or after sleep when behavioural thresholds and suprathreshold sensitivities, suitably defined, are both elevated.

It remains to discuss how the arousal level in pathway 3 of Fig. 20 is modulated by the pacemaker. Is this modulatory action excitatory, inhibitory or disinhibitory? Total ablation of the SCN does not put an animal to sleep (Stephan & Zucker, 1972). Correspondingly, in Fig. 20 the pacemaker cannot be the sole agent of a direct excitatory effect on pathway 3. Two alternative hypotheses are compatible with the data:

(1) Pacemaker output disinhibits a population of tonically active arousal cells which, in turn, excite pathway 3. To model this property, suppose that pacemaker on-cell output inhibits cells which inhibit the tonically active arousal cells, or that pacemaker off-cell output inhibits the tonically active arousal cells.

(2) Pacemaker output both excites and inhibits the population of tonic cells which activate pathway 3. To model this property, let pacemaker on-cell output add to the tonically active level, and pacemaker off-cell output subtract from the tonic level. The tonic level defines a baseline that

can be calibrated to ensure that the motivational dipoles are neither underaroused nor overaroused during the wakeful state.

21. Anticipatory Wheel Turning, Ultradian Feeding Cycles and After-effects of a Single Pulse of Light

When a gated pacemaker circuit, as in Fig. 4, is joined to a motivational circuit, as in Fig. 20, then light can influence the total circuit along several distinct pathways. As an input to the pacemaker, light can act as an external Zeitgeber, as in equations (1d) or (2n), and as a presynaptic gate of slow gain control sensitivity, as in equations (24) or (25). As an input to the motivational circuit, light can act as a reinforcing cue via pathways such as 11 and 12 in Fig. 20.

In much of the circadian literature, reinforcing actions of external cues such as light are not explicitly analysed. In situations where light is left on for long periods of time, one can argue that reinforcing factors are less important than circadian factors due to the long time scale of the light-mediated events. Even in cases where light does act like a negative conditioned reinforcer within a nocturnal model, its suppressive effects as a conditioned reinforcer (Grossberg, 1972*a*,*b*, 1982*c*) can often parallel its suppressive effects as a Zeitgeber. These two actions of light may be difficult to dissociate.

It is less easy to ignore the reinforcing action of light in the explanation of behaviors that can be induced on a single trial, or behaviors that are anticipatory in nature. Under these circumstances, reinforcement mechanisms may interact with circadian mechanisms in a complex fashion. For example, in the generation of after-effects by a single intense pulse of light (Pittendrigh, 1960), light may act as a punishing stimulus in addition to acting like a Zeitgeber. Such a punishing event may influence the conditioned reinforcing properties of situational cues in a manner that is difficult to determine without experimental controls. A change in the conditioned reinforcing properties of situational cues could, in turn, phase shift or otherwise change the animal's behavioral repertoire.

In a similar fashion, the eating cycle can be phase shifted by presenting food-related conditioned reinforcing cues. The direct phase-shifting action of these cues can phase shift the onset of the satiety signal. The phase-shifted satiety signal can, in turn, help to phase shift the subsequent eating cycle. This is because the satiety signal can maintain an ultradian eating cycle, even in the absence of a circadian pacemaker, just so long as food and other reinforcers are constantly available.

These remarks indicate the need to join together concepts about circadian rhythms with concepts about reinforcement and motivated behavior. The properties of gated dipole circuits provide a formal language with which to expedite this synthesis.

22. Intracellular Gated Dipoles: Photoreceptors and Pacemakers

The discussion in Sections 19 and 20 shows that the formal properties of gated dipole circuits may be specialized to generate different behavioral properties. This section points out that the same formal gated dipole circuit can, in principle, be realized biologically in many different ways. To build the basic pacemaker of Fig. 4, all one needs are opponent processes, habituating transmitter gates, a tonic metabolic source, and appropriately wired feedback pathways. All of these requirements can be met at an early phylogenetic stage. Moreover, all of these requirements can, in principle, be realized within a single cell. The opponent processes can be realized by opponent membrane channels in a single cell, in the same way that an Na^+ channel and a K^+ channel are opponent channels in a membrane equation (Carpenter, 1981; Grossberg, 1981*b*). Transmitter gating actions can modulate the sensitivity of these membrane channels on a slow time scale.

Carpenter & Grossberg (1981, 1983*a*) have, in fact, quantitatively simulated parametric data taken from isolated vertebrate photoreceptors using a gated dipole model of the internal transmitter that exists within a single photoreceptor cell. This intracellular transmitter process mediates the transduction of photons into electrical potential (Baylor and Hodgkin, 1974; Baylor, Hodgkin & Lamb, 1974*a*,*b*). The entire gated dipole circuit is hypothesized to occur within a single photoreceptor cell. Spontaneous oscillations do not occur within this model because its circuit is designed to sensitively react to phasic fluctuations in light intensity. A comparison of this gated photoreceptor circuit with a gated pacemaker circuit suggests several ways that a single photoreceptor circuit can be transformed into a pacemaker circuit, or how two or more photoreceptor circuits can be coupled to form a pacemaker circuit.

These formal connections between photoreceptor and circadian models suggest a potentially important new tool for comparative neurological and biochemical studies in this area, since circadian pacemakers exist within certain retinas, such as the *Aplysia* retina (Jacklet, 1969), and the pineal organ, which may be the circadian pacemaker site in birds, is also photoreceptive (Menaker, 1974). In the vertebrate photoreceptor, a Ca^{++} current plays the role of the gating transmitter. It remains to be seen whether a Ca^{++} current plays a gating role in certain primitive circadian pacemakers.

23. Comparison With Other Models

Many circadian models have focussed on the coupling and phasing of two or more oscillators. In these models, the individual pacemakers are chosen for convenience and simplicity, but do not admit a detailed physiological interpretation. For example, the Kronauer *et al.* (1982) and Wever (1962, 1975) models consist of a pair of equations of van der Pol type. The model of Kawato & Suzuki (1980) consists of a pair of coupled FitzHugh-Nagumo equations. As Kawato & Suzuki have noted, "the BVP [van der Pol] equations and Nagumo's equation were derived for neural rhythms with much shorter periods than 24 h. However, in the absence of information regarding the state variables relevant to circadian pacemakers, we use the abstract model" (p. 557). The model of Daan & Berde (1978) describes a pacemaker entirely in terms of its period, phase, and phase shifts. Enright (1980) develops a quasi-neural model in terms of stochastic variables such as the average durations of the discharge phase and the recovery phase, and the amount by which an internal Zeitgeber shortens the average recovery phase. The relationship of the Enright (1980) model to the gated pacemaker model is discussed in detail by Carpenter & Grossberg (1984).

Our analysis complements these contributions concerning the coupling of formal oscillators by explicating the dynamics of a single pacemaker. Figures 4(a) and (b), in particular, do not describe coupled oscillators, but a single oscillator which is hypothesized to occur in many copies within each SCN. Those results about coupled oscillators which are insensitive to the detailed properties of the individual oscillators will carry over to the case where gated pacemakers are the oscillators to be coupled.

Our results indicate, however, that many properties, such as split rhythms and after-effects, which have heretofore been assumed to require coupling between oscillators can be explained by internal properties of a single oscillator. We also suggest a new explanation of the effects of parametric and nonparametric lighting regimes. These claims do not deny the existence of coupling between distinct sleep and temperature systems (Kronauer *et al.*, 1982; Wever, 1979). Nor do they deny the existence of distinct pacemakers in each SCN that may, under certain circumstances, drift out of phase. Rather we show how data properties which cannot be explained by classical oscillators unless they are allowed to drift out of phase can be explained by a population of gated pacemaker oscillators that remain in phase. At the very least, our results point out those areas where futher argument is needed to conclude that a coupling between out-of-phase oscillators generates a data property.

Previous circadian models explain split rhythms by describing how two oscillators, or two populations of oscillators, can drift out of phase under

certain conditions (Daan & Berde, 1978; Enright, 1980; Kawato & Suzuki, 1980; Pavlidis, 1973; Pittendrigh, 1960; Pittendrigh & Daan, 1976*b*; Wever, 1984; Winfree, 1967). Models of this type simulate after-effects as long-term transients that persist subsequent to initial phasing differences between constituent oscillators (Daan & Berde, 1978; Enright, 1980). The long-term nature of these transients is due to the weakness of the coupling whereby constituent oscillators mutually influence each other. None of these approaches provides a unified explanation of the data base that the gated pacemaker model has simulated in this and previous articles.

A notable difficulty arises in simulating both parametric (LL) and non-parametric (LD) after-effects (section 3). For example, the sequence of models developed by Pittendrigh (1974), Pittendrigh & Daan (1976*b*), and Daan & Berde (1978) assumes that separate mechanisms process parametric and non-parametric lighting regimes. A parametric lighting regime induces a change in model parameters, such as oscillator periods or coupling strengths. In a nonparametric lighting regime, light onset or offset phase-resets both of the model oscillators, but has no effect on model parameters. In section 2, we noted that all lighting regimes are nonparametric at the pacemaker. In the Daan & Berde (1978) model, by contrast, internal light onset and offset due to waking and sleeping in LL have no phase-resetting properties (p. 305), and the 18 hours of light experienced during LD 18:6 have no effects on model parameters (p. 309). By extension, LD 23.9:0.1 would have no effects on model parameters, but LL ≡ LD 24:0 would.

Many of the difficulties that arise when classical oscillators are used to model circadian data are eliminated by using the physiologically motivated gated pacemaker design. Future work may show that a synthesis of recent concepts concerning physiologically characterized individual oscillators with classical concepts concerning the phasing of oscillators may explain an even larger data base. For example, in our explanation of split rhythms, a reduction in the level of fatigue feedback occurs in LL. This reduction could allow individual gated pacemakers to drift out-of-phase, in a manner more in tune with other explanations. Simulations of gated pacemaker populations may shed further light on the transitional activity patterns which occur prior to a fully split rhythm.

Independent of such considerations, the gated pacemaker model introduces several types of processes into the circadian literature which may prove to be important in future theories: a possible role for chemical gating actions and on-cell off-cell interactions in a circadian pacemaker, homeostatic ultradian feedback signals, slowly gating nonhomeostatic feedback signals, and rapidly acting nonhomeostatic signals, such as light, whose mode of action upon the pacemaker is distinguished from their strength at the environmental source.

The authors thank Cynthia Suchta for her valuable assitance in the preparation of the manuscript and illustrations.

REFERENCES

ASCHOFF, J. (1954). *Naturwissenschaften* **41**, 49.
ASCHOFF, J. (1960). *Cold Spring Harbor Symp. Quant. Biol.* **25**, 11.
ASCHOFF, J. (1979). *Z. Tierpsychologie* **49**, 225.
BAYLOR, D. A. & HODGKIN, A. L. (1974). *J. Physiol.* **242**, 729.
BAYLOR, D. A., HODGKIN, A. L. & LAMB, T. D. (1974a). *J. Physiol.* **242**, 685.
BAYLOR, D. A., HODGKIN, A. L. & LAMB, T. D. (1974b). *J. Physiol.* **242**, 759.
BORBÉLY, A. A. (1982). *Human Neurobiol.* **1**, 195.
CARD, J. P., RILEY, J. N. & MOORE, R. Y. (1980). *Neuroscience Abst.* **6**, 758.
CARPENTER, G. A. (1981). In: *Mathematical psychology and psychophysiology.* (Grossberg, S. ed.). pp. 49-90. Providence, RI: Amsterdam Mathematical Society.
CARPENTER, G. A. (1983). In: *Synergetics of the Brain.* (Basar, E., Flohr, H., Haken, H. & Mandell, A. J. eds). pp. 311-329. Berlin: Springer-Verlag.
CARPENTER, G. A. & GROSSBERG, S. (1981). *J. theor. Neurobiol.* **1**, 1.
CARPENTER, G. A. & GROSSBERG, S. (1982). *Neuroscience Abst.* **8**, 546.
CARPENTER, G. A. & GROSSBERG, S. (1983a). In: *Oscillations in mathematical biology.* (Hodgson, J. P. E. ed.). pp. 102-196. Berlin: Springer-Verlag.
CARPENTER, G. A. & GROSSBERG, S. (1983b). *Biol. Cybernet.* **48**, 35.
CARPENTER, G. A. & GROSSBERG, S. (1984). *Am. J. Physiol.* **247**, R1067.
CZEISLER, C. A., WEITZMAN, E. D., MOORE-EDE, M. C., ZIMMERMAN, J. C. & KRONAUER, R. S. (1980). *Science*, **210**, 1264.
DAAN, S. & BERDE, C. (1978). *J. theor. Biol.* **70**, 297.
DAAN, S. & PITTENDRIGH, C. S. (1976). *J. Comp. Physiol.* **106**, 253.
DECOURSEY, P. J. (1960). *Cold Spring Harbor Symp. Quant. Biol.* **25**, 49.
EARNEST, D. & TUREK, F. W. (1982). *J. Comp. Physiol.* **145**, 405.
EARNEST, D. & TUREK, F. W. (1983). *Neuroscience Abst.* **9**, 626.
ENRIGHT, J. T. (1980). *The timing of sleep and wakefulness.* Berlin: Springer-Verlag.
GREEN, D. J. & GILLETTE, R. (1982). *Brain Res.* **245**, 198.
GROOS, G. A. (1982). *Vertebrate circadian systems.* (Aschoff, J., Daan, S. & Groos, G. A. eds). pp. 96-105. Berlin: Springer-Verlag.
GROOS, G. A. & HENDRIKS, J. (1979). *Experientia* **35**, 1597.
GROOS, G. A. & HENDRIKS, J. (1982). *Neurosci. Lett.* **34**, 283.
GROOS, G. A. & MASON, R. (1978). *Neurosci. Lett.* **8**, 59.
GROOS, G. A. & MASON, R. (1980). *J. Comp. Physiol.* **135**, 349.
GROSSBERG, S. (1968). *Proc. natn. Acad. Sci. U.S.A.* **60**, 758.
GROSSBERG, S. (1969). *J. theor. Biol.* **22**, 325.
GROSSBERG, S. (1972a). *Math. Biosci.* **15**, 39.
GROSSBERG, S. (1972b). *Math. Biosci.* **15**, 253.
GROSSBERG, S. (1975). *Int. Rev. Neurobiol.* **18**, 263.
GROSSBERG, S. (1978). In: *Progress in theoretical biology*, vol. 5. (Rosen, R. & Snell, F. eds). pp. 233-274.
GROSSBERG, S. (1980). *Psychol. Rev.* **87**, 1.
GROSSBERG, S. (1981a). In: *Mathematical psychology and psychophysiology.* (Grossberg, S. ed.). pp. 157-186. Providence, RI: American Mathematical Society.
GROSSBERG, S. (1981b). In: *Mathematical psychology and psychophysiology.* (Grossberg, S. ed.). pp. 107-156. Providence, RI: American Mathematical Society.
GROSSBERG, S. (1982a). *Studies of mind and brain: Neural principles of learning, perception, development, cognition, and motor control.* Boston: Reidel Press.
GROSSBERG, S. (1982b). *Psychol. Rev.* **89**, 529.

GROSSBERG, S. (1982c). *J. theor. Neurobiol.* **1**, 286.
GROSSBERG, S. (1984a). In: *Brain and information: Event related potentials.* (Karrer, R., Cohen, J. & Tueting, P. eds). pp. 58–151. New York: New York Academy of Sciences.
GROSSBERG, S. (1984b). *Biol. Psychiatry* **19**, 1075.
GROSSBERG, S. (1984c). In: *Perception of speech and visual form: Theoretical issues, models, and research.* (Schwab, E. C. & Nusbaum, H. C. eds). New York: Academic Press.
GROSSBERG, S. (1985). In: *Temporal Order.* (Rensing, L. ed.). New York: Springer-Verlag.
GWINNER, E. (1974). *Science* **185**, 72.
HEDBERG, T. G. & MOORE-EDE, M. C. Circadian rhythmicity in multiple-unit activity of rat hypothalamic slice. *Neuroscience Abst.* **9**, 1068.
HODGKIN, A. L. (1964). *The conduction of the nervous impulse.* Liverpool: Liverpool University.
HODGKIN, A. L. & HUXLEY, A. F. (1952). *J. Physiol.* **117**, 500.
HOFFMANN, K. (1971). In: *Biochronometry.* (Menaker, M. ed.). pp. 134–150. Washington, DC: National Academy of Sciences.
INOUYE, S. T. & KAWAMURA, H. (1979). *Proc. natn. Acad. Sci. U.S.A.* **76**, 5962.
IUVONE, P. M., BESHARSE, J. C. & DUNIS, D. A. (1983). *Neuroscience Abst.* **9**, 624.
JACKLET, J. (1969). *Science* **164**, 562.
KATZ, B. (1966). *Nerve, muscle, and synapse.* New York: McGraw-Hill.
KAWATO, M. & SUZUKI, R. (1980). *J. theor. Biol.* **86**, 547.
KRAMM, K. R. (1971). *Circadian activity in the antelope ground squirrel Ammospermophilus leucurus.* Ph.D. Thesis, University of California at Irvine.
KRONAUER, R. E., CZEISLER, C. A., PILATO, S. F., MOORE-EDE, M. C. & WEITZMAN, E. D. (1982). *Am. J. Physiol.* **242**, R3.
KUFFLER, S. W. & NICHOLLS, J. G. (1976). *From neuron to brain.* Sunderland, MA: Sinauer Press.
LIN, C. C. & SEGEL, L. A. (1974). *Mathematics applied to deterministic problems in the natural sciences.* New York: Macmillan Publishing Company.
LINCOLN, D. W., CHURCH, J. & MASON, C. A. (1975). *Acta Endocrinol.* (supplement), **199**, 184.
MENAKER, M. (1974). In: *Circadian oscillations and organization in nervous systems.* (Pittendrigh, C.S. ed.). pp. 479–489. Cambridge, MA: MIT Press.
MOORE, R. Y. (1973). *Brain Res.* **49**, 403.
MOORE, R. Y. (1974). In: *Circadian oscillations and organization in nervous systems.* (Pittendrigh, C. S. ed.). pp. 537–542. Cambridge, MA: MIT Press.
MOORE, R. Y., CARD, J. P. & RILEY, J. N. (1980). *Neuroscience Abstr.* **6**, 758.
MOORE, R. Y. & EICHLER, V. B. (1972). *Brain Res.* **42**, 201.
MOORE-EDE, M. C., SULZMAN, F. M. & FULLER, C. A. (1982). *The clocks that time us.* Cambridge, MA: Harvard University Press.
NISHINO, H., KOIZUMI, K. & BROOKS, C. M. (1970). *Brain Res.* **112**, 45.
OLDS, J. (1977). *Drives and reinforcements: Behavioral studies of hypothalamic function.* New York: Raven Press.
PAVLIDIS, T. (1973). *Biological oscillators: Their mathematical analysis.* New York: Academic Press.
PICKARD, G. E. & TUREK, F. W. (1982). *Science* **215**, 1119.
PITTENDRIGH, C. S. (1960). *Cold Spring Harbor Quant. Biol.* **25**, 159.
PITTENDRIGH, C. S. (1974). In: *Circadian oscillations and organization in nervous systems.* (Pittendrigh, C. S. ed.). pp. 437–458. Cambridge, MA: MIT Press.
PITTENDRIGH, C. S. & DAAN, S. (1976a). *J. comp. Physiol.* **106**, 223.
PITTENDRIGH, C. S. & DAAN, S. (1976b). *J. comp. Physiol.* **106**, 333.
PITTENDRIGH, C. S. & MINIS, D. H. (1964). *Am. Nat.* **98**, 261.
PLONSEY, R. (1969). *Bioelectric phenomena.* New York: McGraw-Hill.
POHL, H. (1982). In: *Vertebrate circadian systems.* (Aschoff, J., Daan, S. & Groos, G. A. eds). pp. 339–346. Berlin: Springer-Verlag.
SATO, T. & KAWAMURA, H. (1984). *Neurosci. Res.* **1**, 45.
SCHWARTZ, W. J., DAVIDSEN, L. C. & SMITH, C. B. (1980). *J. comp. Neurol.* **189**, 157.

SCHWARTZ, W. J. & GAINER, H. (1977). *Science* **197**, 1089.
SCHWARTZ, W. J., REPPERT, S. M., EAGAN, S. M. & MOORE-EDE, M. C. (1983). *Brain Res.* **274**, 184.
SHIBATA, S., OOMURA, Y., KITA, H. & HATTORI, K. (1982). *Brain Res.* **247**, 154.
STEPHAN, F. Y. & ZUCKER, I. (1972). *Proc. natn. Acad. Sci. U.S.A.* **69**, 1583.
TERMAN, M. & TERMAN, J. (1983). *Neuroscience Abst.* **9**, 1071.
WEVER, R. (1962). *Kybernetik* **1**, 139.
WEVER, R. (1975). *Int. J. Chronobiol.* **3**, 19.
WEVER, R. (1979). *The circadian system of man: Results of experiments under temporal isolation.* Berlin: Springer-Verlag.
WEVER, R. (1984). *Mathematical models of the circadian sleep-wake cycle.* (Moore-Ede, M. C. & Czeisler, C. A. eds). pp. 17-77. New York: Raven Press.
WINFREE, A. T. (1967). *J. theor. Biol.* **16**, 15.

APPENDIX

Choice of parameters

This section describes the parameter choices that were used in the nocturnal model equations (1n), (2n), (3)-(6). These equations are already almost in dimensionless form (Lin & Segel, 1974). In general, converting a full system of equations to dimensionless form eliminates as many parameters as there are dependent and independent variables. The nocturnal model contains six dependent variables (x_1, x_2, z_1, z_2, F, y) and one independent variable (t). The nocturnal model equations already contain six fewer parameters than could have been used to describe this system. Coefficients have been eliminated in front of the terms $f(x_1)z_1$ and $g(x_2)$ in equation (1n), the terms $f(x_2)z_2$, F, and $g(x_1)$ in equation (2n), and term V in equation (6). Recall that the functions f, g, and V are all scaled to vary between 0 and 1. It remains to eliminate one more parameter. Dimensional analysis of the nocturnal model shows that the parameter A can be used to fix the time scale of the model. Thus some model parameters are expressed below as multiples of A. These multiples contain physical information about relative sizes and speeds. A fixed choice of A determines the time scale without altering these relative relationships.

Alternate versions of the model were used for illustrative purposes in Figs 1(b) and 5. In all other simulations described in the article, the following parameters were always constant ratios of A

$$B = 5A, \tag{A1}$$

$$C = 0{\cdot}5A, \tag{A2}$$

$$D = 0{\cdot}01A, \tag{A3}$$

$$E = 0{\cdot}4, \tag{A4}$$

$$H = 0{\cdot}02, \tag{A5}$$

$$I = 0{\cdot}1A, \tag{A6}$$

$$K = 0{\cdot}17A, \tag{A7}$$

$$N = 0{\cdot}72A, \tag{A8}$$

$$P = 0{\cdot}665A, \tag{A9}$$

$$R = 0{\cdot}0001A, \tag{A10}$$

$$W = 100A^{-1}, \tag{A11}$$

$$\theta = 0{\cdot}5. \tag{A12}$$

Carpenter & Grossberg (1983*b*) provide a detailed analysis of how parameters can be chosen within a wide parameter range to generate physically plausible oscillations in the absence of fatigue and slow gain control. This 4-dimensional system is called the basic gated pacemaker. Our focus in the present article has been to understand how the fatigue and slow gain control processes modulate the properties of the basic gated pacemaker. We therefore chose the relative sizes of the equations (A1)-(A12) once and for all based on the Carpenter & Grossberg (1983*b*) analysis and focussed our attention upon how to choose fatigue and slow gain control parameters. Other parametric ranges in Carpenter & Grossberg (1983*b*) could also have been used to generate similar results.

The following relative sizes are physically important in the model. By equations (A1) and (A2),

$$C/B = 0{\cdot}1. \tag{A13}$$

In equations (1n) and (2n), parameters B and C are the excitatory saturation point (V_{Na}) and inhibitory saturation point (V_K) of their respective potentials. The ratio $V_K/V_{Na} \cong 0{\cdot}1$ in many cells (Hodgkin & Huxley, 1952). The ratio

$$K/A = 0{\cdot}17 \cong \tfrac{1}{6} \tag{A14}$$

in equation (A7) is also physically interesting. By equation (5), equation (A7) says that fatigue decays on an ultradian time scale of approximately $\frac{1}{6}$ of a day. By equations (A8) and (A9), the activity threshold N is always chosen larger than the sleep threshold P.

Carpenter & Grossberg (1983*b*) show that the order of magnitude of the circadian period in the basic gated pacemaker is $1/D$. By equations (A3) and (A10),

$$R/D = 0{\cdot}01. \tag{A15}$$

Parameter R is the decay rate of the slow gain control process y in equations

(18), (24), and (27)-(29). By equation (A15), y decays on a time scale of months ($\cong 100$ days).

Parameter W in equation (A11) was chosen large so that light significantly attenuates S_{light} in equation (23). Choosing parameter $\theta = 0{\cdot}5$ in equation (A12) says that a 50% attenuation of light intensity occurs during sleep, due to equation (13).

All the parameters in equations (A1)-(A12) are specified by a choice of the single parameter A. In all the after-effect simulations, we chose

$$A = \tfrac{113}{24} \cong 4{\cdot}7083. \tag{A16}$$

In all the split rhythm simulations, we chose

$$A = \tfrac{144}{24} = 6. \tag{A17}$$

These choices of A determine the time scale in hours. This conclusion follows from the fact, demonstrated in Carpenter & Grossberg (1983*b*), that the order of magnitude of the *dimensionless* circadian period in the basic gated pacemaker is A/D. By equation (A3),

$$A/D = 100. \tag{A18}$$

Since the order of magnitude of the circadian period in equations (1)-(6) is $1/D$, to get $1/D \cong 24$ hours, it follows by equation (A18) that choices of $A \cong 100/24$, as in equations (A16) and (A17), determine the unit of time to be hours.

Only parameters M and Q remain to be specified. The choice of M in equation (8) determines the magnitude of the fatigue signal in equations (2) and (5). In all after-effect simulations, we chose

$$M = 0{\cdot}01A. \tag{A19}$$

In all split rhythm simulations, we chose

$$M = 0{\cdot}028A. \tag{A20}$$

Parameter Q determines the magnitude of the performance signal S in equation (1). In all split rhythm simulations, $S = QS_{\text{awake}}$, and we chose

$$Q = 6{\cdot}4 \times 10^{-6}A. \tag{A21}$$

In the after-affect simulations, we showed that more than one choice of S could simulate the data. For the gain control process defined by equations (14)-(16) and shown in Fig. 13, we chose

$$Q = 1{\cdot}4 \times 10^{-6}A. \tag{A22}$$

For both of the other gain control processes used to simulate after-effects

(Fig. 16), we chose

$$Q = 2{\cdot}8 \times 10^{-6} A. \tag{A23}$$

In equation (13), the light $L(t)$ is either on or off. "Bright light" is experimentally defined to be an intensity somewhat less than the intensity at which wheel turning ceases in constant light (LL). We chose light intensity in a similar way by using intensities somewhat smaller than those intensities at which $x_1(t)$ remains less than the activity threshold N in LL.

It remains only to say how the initial data of x_1, x_2, z_2, F, and y were chosen at time $t = 0$. The simulations were insensitive to the initial values of x_1, x_2, z_1, z_2, and F. Due to its slow time scale, $y(0)$ was chosen in each case at its equilibrium value in the dark (DD).